理學博士 學位論文

Regulation of E-cadherin Junctions by the c-Jun N-terminal Kinase in Oral Keratinocytes

c-Jun N-말단 인산화효소에 의한 구강각화세포의 E-cadherin 결합 조절

2017년 8월

서울대학교 대학원

치의과학과 세포및발생생물학 전공

이 가 영

ABSTRACT

Regulation of E-cadherin Junctions by the c-Jun N-terminal Kinase in Oral Keratinocytes

Ga young Lee

Department of Cell & Developmental Biology

School of Dentistry

The Graduate School

Seoul National University

Maintaining cell-cell adhesions of keratinocytes is crucial in tightly packing the cells in the epithelium and protecting tissues underlying epithelium against harmful agents such as microorganisms or toxins. E-cadherin junctions (ECJs) have a major role in keeping the integrity of adhesion complex of oral keratinocytes. Therefore understanding of the molecular mechanisms of their formation is critical in both normal and transformed oral keratinocytes. First, HOK-16B cells, a normal human gingival epithelial cell line, were used to identify the molecules involved in the regulation of the formation of intercellular E-cadherin junctions between human gingival

epithelial cells. Activation of c-Jun N-terminal kinase (JNK) disrupted the intercellular junctions through the dissociation of E-cadherin. The role of JNK in the formation of these E-cadherin junctions was further confirmed by demonstrating that JNK inhibition induced the formation of intercellular E-cadherin junctions. The upstream signaling of JNK was also examined. Activation of the small GTPase RhoA disrupted the formation of E-cadherin junctions between HOK-16B cells, which was accompanied by JNK activation. Disruption of these intercellular junctions upon RhoA activation was prevented when JNK activity was inhibited. In contrast, RhoA inactivation led to HOK-16B cell aggregation and the formation of intercellular junctions, even under conditions in which the cellular junctions were naturally disrupted by growth on a strongly adhesive surface. Then, the JNK-dependent regulation of E-cadherin junction was confirmed in gingival epithelium including junctional epithelium (JE) of which intercellular junction is poorly formed. Expectedly, JE of mouse molars had high JNK activity associated with low E-cadherin expression, which was reversed in the other gingival epithelia, including the sulcular epithelium. Next, the molecular mechanism by which squamous cell carcinoma cells grow scattered at the early phase of transformation while maintaining the epithelial phenotype was studied because cell scattering of epithelial carcinoma cancer cells is one of the critical event in tumorigenesis. Cells losing epithelial cohesion detach from aggregated epithelial cell masses and

may migrate to fatal organs through metastasis. YD-10B cells which are established from human oral squamous cell carcinoma was studied because the cells grow scattered without the formation of ECJs under routine culture conditions despite the high expression of functional E-cadherin. The functionality of their E-cadherin was demonstrated in that YD-10B cells formed ECJs, transiently or persistently, when they were cultured on substrates coated with a low amount of fibronectin or to confluence. The phosphorylation of JNK was up-regulated in YD-10B cells compared with that in human normal oral keratinocyte cells or human squamous cell carcinoma cells, which grew aggregated along with well-organized ECJs. The suppression of JNK activity induced the aggregated growth of YD-10B cells concomitant with the development of ECJs. These results indicate that the decreased formation of intercellular E-cadherin junctions between human gingival keratinocytes may be coupled to high JNK activity and the inherently up-regulated JNK activity induces the scattered growth of the oral squamous cell carcinoma cells through disassembly of ECJ despite the expression of functional E-cadherin, a hallmark of the epithelial phenotype.

Key word: E-cadherin, JNK, RhoA, oral gingival epithelial cell, oral squamous cell carcinoma cell.

Student Number: 2011-23828

TABLE OF CONTENTS

LIST OF FIGURES

ABBREVIATIONS

ECJ	E-cadheriun junction
JE	junctional epithelium
GE	gingival epithelium
SE	sulcular epithelium
HOK	human oral keratinocyte
HGK	human gingival keratinocyte
JNK	c-Jun N-terminal kinase
ODAM	odontogenic ameloblast-associated protein
FITC	fluorescein isothiocyanate
DAPI	4′,6-diamidino-2-phenylindole dihydrochloride
MLC	myosin light chain
FN	fibronectin
MKK-JNK1	pCS-CG-MKK7b2-JNK1a1
MKK-JNK2	pCS-CG-MKK7b2-JNK2a2
CNT	carbon nanotube
shRNA	small hairpin RNA
S	smooth substrate
R	rough substrate

Ra	average roughness
R(4000)	prepared with #4000 sandpaper
EMT	epithelial–mesenchymal transition

CHAPTER I

GENERAL INTRODUCTION

1. E-Cadherin

E-cadherin also called as cadherin-1 or CAM 120/80 is a protein encoded by the CDH1 gene which is a tumor suppressor gene [1-3]. E-cadherin is a cell-cell adhesion glycoprotein which is calcium-dependent. It is expressed in various epithelial cells including oral keratinocytes [4]. It contributes to the formation of an epithelial barrier sealing the intercellular junction against the invasion of microorganisms or toxins The extracellular domain of E-cadherin mediates bacterial adhesion to epithelial cells [5]. The intracellular domain has a highly-phosphorylated region which is critical in β-catenin binding to E-cadherin. α-catenin binding to β-catenin play a part in regulating the assembly of F-actins [6]. Mutations in this gene are associated with various epithelial cancers such as breast, gastric, colorectal, ovarian, and thyroid cancers. Loss of function of E-cadherin increases proliferation, invasion, and/or metastasis which contribute to the cancer progression and metastasis. Down-regulation of E-cadherin expression decreases the strength of cell-cell adhesion, resulting in an increased cellular motility [7-11].

2. c-Jun N-terminal kinases (JNKs)

The c-Jun N-terminal kinases (JNKs) are a member of the mitogen-activated protein kinase family. They are activated in responses to various stress stimuli, such as ultraviolet irradiation [12], cytokines[13], osmotic

shock [14], reactive oxygen species, inflammatory signals, protein synthesis inhibitors, and heat shock [15, 16]. Inhibition of phosphatases also inhibit the activity of JNK and its downstream. They are associated with the pathways involving in cellular apoptosis and T cell differentiation. JNKs are activated through a dual phosphorylation of threonine and tyrosine residues in kinase subdomain VIII by MKK4 or MKK7. Ser/Thr or Tyr protein phosphatases inactivates JNKs [17]. Ten JNKs isoforms of 46 kDa or 55 kDa are derived from three genes: four isoforms of JNK1, four isoforms of JNK2 and two isoforms of JNK3. Both JNK1 and JNK2 are expressed in all cells and tissues, whereas JNK3 is found in the brain, heart, and the testes [18, 19].

3. Ras homolog gene family, member A (RhoA)

Ras homolog gene family, member A (RhoA), a small GTPase, is one of Rho family. Active RhoA regulates cytoskeleton, especially development of actin stress fibers and contractility of actomyosin. In addition, RhoA activity is associated with cell cycle progression, transcription, and cell transformation. RhoA is activated by various guanine nucleotide exchange factors (GEFs) through phosphorylation [20]. The GTP-bound RhoA through exchanging of GDP to GTP activates RhoA. There are several effectors of RhoA including ROCK1 (Rho-associated, coiled-coil containing protein kinase 1) and DIAPH1 (Diaphanous Homologue 1, a.k.a. hDia1, diaphanous in Drosophila, homologue to mDia1 in mouse). Activated RhoA stimulates Rho-associated

kinase (ROCK) – LIM kinase which then activates cofilin. Next, cofilin reorganizes the F-actin. Among various functions involved in RhoA activity, RhoA directly polymerizes F-actin through the activation of mDia1. ROCK contracts actomyosin through regulating myosins and various actin-binding proteins, which regulating cell migration and detachment [21]. RhoA activity is also associated with cell-cell adhesions, primarily in adherens or tight junctions [22, 23].

4. Gingival junctional epithelium

Junctional epithelium (JE) seals the interface between the oral cavity and the underlying connective tissue. JE is unique in that it contacts with the solid surface of the tooth. It is a junction of a potential weakness through which bacterial products enter the connective tissue eliciting inflammation. JE is localized under the bottom of the gingival sulcus to the tooth apex. Epithelium of JE is different from those of the sulcus. Oral sulcular epithelium is lined by typical oral epithelium which is a nonkeratinized stratified squamous epithelium of tight intercellular junction. However, JE is a nonkeratinized stratified squamous epithelium of loose intercellular junction which contacts both lamina propria of gingiva and tooth surface simultaneously [24-26]. The cells in the JE uniquely presents a morphology of incompletely differentiated epithelium. Tonofilaments and desmosomal junctions in the JE cells are fewer. K5, K8, K14, K18, K19 cytokeratins are found in the JE cells which are localized in

basal epithelial cells or simple epithelia [27, 28]. In addition, striking wide intercellular space may be associated with the permeability of JE, which may explain the presence of infiltrating leukocytes in JE [25].

5. Purpose of this study

The main purpose of this study is to investigate the signaling mechanisms to identify the regulation of development of intercellular junctions in oral gingival keratinocytes and oral squamous carcinoma cells. To achieve this goal, I examined the effect of controlling the formation of the E-cadherin junctions 1) regulated by the interaction between RhoA and JNK signaling on fibronectin smooth/rough surface in normal oral keratinocytes, and 2) in oral squamous cell carcinoma (OSCC) cells. Next, I verified the differences of the signaling regulations between normal oral keratinocytes and carcinoma cells. Finally, I detected to establish a model cell line, which grow scattered affected by the activity of the JNK, YD-10B oral squamous cell carcinoma.

Chapter Ⅱ

RhoA-JNK Regulates the E-Cadherin Junctions of Human Oral Keratinocytes

* This chapter has been largely reproduced from an article published by Lee, G.Y., Kim H.J., and Kim H.M. (2016) Journal of Dental Research, 95(3), 284-291. and by Lee G.Y., Jin C.B. and Kim H.M. (2017) Journal of Periodontal Implant Science, 47(2), 116-131.

i. INTRODUCTION

The junctional epithelium (JE) forms a seal between tooth and gingiva, where it functions as a barrier against attack by microorganisms or toxic substances [25, 26]. However, the JE does not provide an appropriate protective epithelial barrier due to its structure. Its intercellular junctions are poorly developed and sparse, and its intercellular space is wide compared with that of the gingival epithelium (GE), which is tightly packed with well-developed intercellular junctions. Thus, bacterial toxins or bacteria may invade these wider spaces, resulting in gingivitis. If bacteria further invade this vulnerable barrier, the barrier will be irreversibly destroyed through induction of subepithelial inflammation. Here, the inflammatory response in connective tissue produces inflammatory cytokines, which further deteriorate the epithelial defense barrier established by the JE. Therefore, understanding the mechanisms that maintain the structural integrity of the JE is essential in preventing and treating gingivitis and periodontitis.

The structural weakness of the intercellular junctions within the JE suggests that the mechanism regulating these junctions is defective. In this study, the molecular features associated with the development of intercellular E-cadherin junctions were analyzed to determine what factors lead to the poor development of intercellular junctions between oral keratinocytes. E-cadherin is the major adhesion molecule connecting epithelial cells within the JE [29] and is localized at the desmosome of the epithelium [30-33], which provides

strong adhesion between epithelial cells. In addition, E-cadherin is regarded as a crucial molecular component within the organization of the desmosomal molecular complex [30-33]. For example, the E-cadherin-plakoglobin complex is required for desmosome organization [34]. E-cadherin is also critical in maintaining the structural integrity of the oral epithelium [26, 29]. Recently, c-JUN NH3-terminal kinase (JNK) was shown to be involved in negatively regulating the formation of intercellular E-cadherin junctions [35, 36]. Active JNK phosphorylates β-catenin to prevent E-cadherin complexes from forming. In the present study, human oral keratinocytes were analyzed to determine whether the formation of their intercellular E-cadherin junctions is dependent on JNK activity and which molecular control mechanisms regulate this activity. Understanding the molecular mechanisms controlling the formation of intercellular junctions between oral epithelial keratinocytes may provide insight into the poor development of these junctions and ways in which to ultimately defend against bacterial diseases in the oral cavity.

ii. MATERIALS AND METHODS

1. Reagents

The following antibodies for Western blotting were purchased from Cell Signaling Technology (Danvers, MA, USA): rabbit anti-JNK, rabbit anti-phospho-JNK (Thr183/Tyr185), rabbit anti-E-cadherin, rabbit anti-GAPDH, and HRP-linked anti-rabbit IgG. Anti-phospho-myosin light chain (p-MLC) was purchased from Millipore (Darmstadt, Germany). Rabbit anti-E-cadherin and rabbit anti-phospho-JNK for immunocytochemistry studies were also obtained from Cell Signaling Technology. Cy™3-conjugated AffiniPure goat anti-rabbit IgG (H+L) (Cy3-IgG) was purchased from Jackson Immunoresearch Laboratories (West Grove, PA, USA). Antiserum against odontogenic ameloblast-associated protein (ODAM) (Nishio et al. 2010) was a gift from Dr. Joo-Cheol Park (Seoul National University, Seoul Korea). SP600125 (JNK inhibitor), SB203580 (p38 inhibitor), U0126 (ERK inhibitor), fluorescein isothiocyanate-labeled phalloidin (phalloidin-FITC), and 4′,6-diamidino-2-phenylindole dihydrochloride (DAPI) were obtained from Sigma-Aldrich (St. Louis, MO, USA). Exoenzyme C3 transferase from Clostridium Botulinum (C3; RhoA inhibitor) and CNF-1 (RhoA activator) were obtained from Cytoskeleton (Denver, CO, USA). Col-Tgel was purchased from 101Bio (Palo Alto, CA, USA).

2. Preparation of culture dish surfaces

Two different concentrations of fibronectin (Sigma-Aldrich) were used to coat hydrophobic petri dishes to allow for HOK-16B cell growth as a typical confluent epithelial layer (0.1 μg/cm2 fibronectin) or as a scattered cell layer (1 μg/cm2 fibronectin) at 37℃ for 2 h. Laminin (Engelbreth-Holm-Swarm murine sarcoma basement membrane, Sigma-Aldrich; 1 μg/cm2) was also coated onto the dishes for the scattered cell growth experiments. Dishes were then washed with PBS, blocked with 5% BSA for 1 h at 37℃, washed again with PBS, and kept at 4℃ until use. Collagen gel surfaces were prepared by pouring a mixture of Col-Tgel component A and component B (20:1 v/v) onto culture dishes and incubating at 37℃ for 45 min. Solidified gel surfaces were coated with 1 μg/cm2 of fibronectin for 1 h. Dishes were then washed with PBS.

3. Cell culture

HOK-16B cells from retromolar tissue were a gift from Dr. N-H Park (University of California, Los Angeles, USA) (Park et al. 1991). The cells were grown in KGM keratinocyte growth media supplemented with bovine pituitary extract, GA-1000 (gentamicin, amphotericin-B), hydrocortisone, rhEGF, insulin (recombinant human) (Lonza; Basel, Switzerland), and 1% penicillin.

4. Transfections

pcDNA3-RhoA-Q63L (constitutively active RhoA: RhoA-CA), pcDNA3-RhoA-T19N (dominant-negative RhoA: RhoA-DN), pcDNA3-Flag-MKK7b2-JNK1a1 (constitutively active JNK1), pcDNA3-Flag-MKK7b2-JNK2a2 (constitutively active JNK2), the lentiviral vector pCS-CG were purchased from Addgene (Cambridge, MA, USA). Lipofectamine LTX reagent and Plus™ reagent were purchased from Invitrogen (Carlsbad, CA, USA). Lentiviral vector M1.4, virus packaging vector psPAX2, and envelope protein vector pMD2G were gifts from Dr. Zang-Hee Lee (Seoul National University, Seoul Korea). M1.4-RhoA-CA, M1.4-RhoA-DN, pCS-CG-MKK7b2-JNK1a1, and pCS-CG-MKK7b2-JNK2a2 were generated by Cosmo Genetech (Seoul, Korea). JNK1 shRNA (shJNK1) plasmid for lentiviral transfections was purchased from Santa Cruz Biotechnology (Santa Cruz, CA, USA). HEK293T cells (a gift from Dr. Z-H Lee) were transfected with recombinant vector, psPAX2, and pMD2G simultaneously using Lipofectamine LTX and Plus™ reagents. Lentiviruses generated by the transfected HEK293T cells were used to infect HOK-16B cells. Cells were selected by treating with puromycin.

5. Tissue preparation and immunohistochemistry

All experiments using animals followed protocols approved by the Institutional Animal Care and Use Committee of Seoul National University (SNU-140828-

1). Twelve-week-old C57BL/6 mice were euthanized by asphyxiation in carbon dioxide. Mandibular molars, including surrounding tissues, were excised and fixed with 4% phosphate-buffered paraformaldehyde. Tissues decalcified in a solution of 10% EDTA (pH 7.4) were embedded in paraffin. The deparaffinized sections, treated with a citrate buffer (pH6.0) for antigen retrieval in a microwave oven, were incubated with primary antibodies against E-cadherin or p-JNK overnight at 4℃. These sections were further incubated with Cy3-IgG and examined using a LSM 700 confocal laser-scanning microscope (Zeiss; Oberkochen, Germany). Sections processed without primary antibody treatment were also examined to rule out any non-specific staining.

6. Immunocytochemistry

HOK-16B cells were fixed with 4% w/v paraformaldehyde and permeabilized in 0.5% v/v Triton X-100. The cells were then incubated with primary antibodies against E-cadherin. Finally, cells were treated with Cy3-IgG. F-actin was stained with phalloidin-FITC. Images were acquired using a LSM 700 confocal laser-scanning microscope.

7. Statistical analyses

The data represent the mean ± standard deviation of at least three samples.

Statistical analyses were performed using a t-test for normally distributed data or a signed rank sum test for non-normally distributed data. P values less than 0.05 were considered to be significant.

iii. RESURLTS

1. JNK activity is critical to the formation of intercellular E-cadherin junctions between human oral keratinocytes

HOK-16B cells formed a typical confluent epithelial layer and well-organized junctions expressing a high level of E-cadherin (Fig 1A). We altered JNK activity to determine whether it was required for the formation of E-cadherin junctions between human oral keratinocytes. The pharmacological activation of JNK with anisomycin and the constitutive activation of the MKK7b2-JNK1a1 fusion protein decreased E-cadherin expression at the cell junctions, leading to intercellular dissociations (Fig 1A and B). Treatment of cells with the JNK inhibitor SP600125 prior to treatment with anisomycin eliminated the effect of anisomycin; pretreatment with SB203580, a p38 inhibitor, did not. These results indicate that JNK activity, not p38 activity, disrupts the formation of E-cadherin junctions (Fig 1A). JNK regulation of E-cadherin was further confirmed by demonstrating that the intercellular junctions between HOK-16B cells could be restored by downregulating JNK activity, even in conditions where the cell junctions were naturally disrupted by growth on strongly adhesive surfaces. HOK-16B cells, which had grown scattered on dishes coated with large amounts of laminin or fibronectin (data not shown) and did not develop E-cadherin junctions, formed a typical confluent epithelial layer when JNK activity was inhibited by SP600125 or when cells were

expressed shJNK1 (Fig 1C and D). However, JNK did not regulate the expression level of E-cadherin in these experimental conditions (Fig 6). Moreover, other types of MAPKs, such as ERK and p38, were not associated with the formation of E-cadherin junctions (Fig 7). These results indicate that JNK activity is specifically associated with the formation of intercellular E-cadherin junctions between human oral keratinocytes.

2. RhoA activity disrupts the intercellular junctions between human oral keratinocytes

RhoA controls the dynamics of actin filaments, which are one of the major components of E-cadherin junctions. It has also recently been reported to regulate various essential cell activities, such as proliferation and cell survival, in addition to cell migration and the formation of stress fibers [37-39]. Furthermore, RhoA is reportedly associated with the various functions of cell junctions. Rho GTPases remodel actin-based structures on endothelial cells to facilitate the migration of leukocytes through the junctions between endothelial cells. RhoA activation also increases the permeability of junctions between endothelial cells [40, 41]. Based on these reports, we examined the role of RhoA in regulating the formation of E-cadherin junctions between human oral keratinocytes. CNF-1, a specific RhoA activator, downregulated E-cadherin expression at the intercellular junctions, widening the gaps between neighboring cells (Fig 2A). Constitutive activation of RhoA also

dissociated the cell junctions (Fig 2B). To confirm the function of RhoA as a negative regulator of intercellular junctions, HOK-16B cells growing in a scattered pattern were treated with C3, a specific RhoA inhibitor, in petri dishes coated with a large amount of fibronectin (a highly adhesive surface). Upon treatment with C3, the cells aggregated to form a confluent epithelial layer, accompanied by the formation of intercellular E-cadherin junctions (Fig 2C). The dominant-negative inhibition of RhoA activity also induced cells to develop E-cadherin junctions, even when cultured on a highly adhesive surface (Fig 2D). Taken together, these results indicate that RhoA is a negative regulator of intercellular E-cadherin junctions.

3. RhoA disrupts the intercellular E-cadherin junctions between human oral keratinocytes by activating JNK

RhoA activation induced by treating cells with CNF-1 or by transfecting the cells with a viral vector expressing RhoA-CA upregulated JNK phosphorylation (Fig 3A and B). In contrast, RhoA inhibition induced by treating cells with C3 or by transfecting them with a viral vector expressing RhoA-DN downregulated JNK phosphorylation (Fig 3C and D). Furthermore, disruption of the intercellular junctions resulting from RhoA activation was completely blocked when cells were pretreated with the JNK inhibitor SP600125 (Fig 3E and F). These results suggest that JNK functions at a downstream point in the RhoA signaling pathway to disrupt the intercellular

junctions between human oral keratinocytes.

4. JNK is highly active in junctional epithelial cells, but E-cadherin expression within the intercellular junctions of these cells is low

The p-JNK and E-cadherin expression were detected in the JE and the GE to confirm the presence of an inverse relationship between their expression levels. The JE of mouse molars was identified by the expression of ODAM [42] and by its specific ultrastructural phenotype (Fig 8). Immunohistochemical analysis of the JE showed that the expression level of E-cadherin within the intercellular junctions was substantially lower than that shown for the GE (Fig 4). The low expression of E-cadherin within the JE is common among different species. E-cadherin expression is reported to be lower in the JE in humans as well [29]. As expected, expression levels of p-JNK were higher in the JE than in the GE (Fig 4). These results suggest that higher JNK activity may be associated with the poor development of E-cadherin junctions within the JE.

5. In vitro formation of the intercellular E-cadherin junctions between human oral keratinocytes depends on the stiffness of the underlying surface

The JE is unusual in that it attaches to the surface of enamel, which is the hardest surface in the human body. Attachment to this surface may be enabled through special characteristics of the JE not found in other epithelium. Intercellular junctions between human oral keratinocytes were compared after culturing on flexible collagen gel or in solid polystyrene culture dishes, both of which were coated with a high concentration of fibronectin which disrupt the intercellular junctions. Interestingly, cells cultured on the collagen gels maintained their E-cadherin junctions (Fig 5A). However, HOK-16B cells cultured on the stiff surface of the culture dishes lost their intercellular connections. These results indicate that a stiff surface may induce the activation of a RhoA-JNK signaling pathway that leads to the disruption of the intercellular E-cadherin junctions. As expected, the level of active phosphorylated JNK was higher in cells grown on the stiff culture dishes compared with those grown on the softer collagen surface (Fig 5B). JNK activation by anisomycin disrupted the intercellular E-cadherin junctions formed between cells on the collagen gel surfaces. In contrast, JNK inhibition by SP600125 restored these junctions on the stiff culture dishes. Because RhoA activity could not be directly analyzed due to the cytoskeletal modifications that would occur during cell detachment from the gel matrix, lower RhoA activity on the soft gel surfaces was confirmed by examining the phenotypical changes induced when activating RhoA. RhoA activation by CNF-1 disrupted the intercellular E-cadherin junctions between cells grown on the collagen gel surface. In contrast, RhoA inhibition by C3 restored the junctions

between cells grown in the stiff culture dishes. These results suggest that the stiffness of the surface to which epithelial cells attach and grow may reduce the stability of the intercellular junctions between cells through activation of RhoA-JNK signaling. Thus, it is highly probable that intercellular junctions within the JE are poorly formed as a result of the underlying, highly solid enamel surface.

6. Role of JNK in ECJ development in HGKs cultured on rough surfaces

Cells seeded on the rough surface with mid- (R(4000)) or high-nanometer dimensions (R(1200)) barely developed E-cadherin junctions between cells (Fig 10A). As in above results, JNK was shown to downregulate the ECJ development in HGKs. Therefore, it was examined whether defective ECJ development in the cells cultured on the rough substrates was associated with JNK activity. The expression level of p-JNK was assessed by immunoblotting for p-JNK in cells cultured on substrates with varying levels of roughness. The expression levels of p-JNK were higher in the cells cultured on the rough substrates than in the cells cultured on the smooth substrate (Fig 10E).

JE migrates apically with age. Therefore substrates to which JE attach switch from the smooth enamel surface to the rough cementum surface. Softer cementum surface provides rougher substrates to JE attachment. In addition, deeper scratches made on the soft cementum and dentin by mechanical

periodontal treatments such as root planning or scaling generate much rougher substrates to JE attachment. Thus the development of the intercellular E-cadherin junctions was examined on the rough substrates. As being expected, the highly defective E-cadherin junctions developed concomitant with the increased JNK activity on rough substrates.

Next, the effect of JNK inhibition on ECJ development was examined. The treatment of the cells with SP600125, a pharmacological inhibitor of JNK, clearly promoted ECJ development in the HGKs cultured on the rough substrate with low-nanometer dimensions and on the smooth substrate (Fig 10B). The knockdown of JNK1 or JNK2 via lentiviral transfection of shRNA JNK1 or shRNA JNK2 into the cells also promoted ECJ development in HGKs cultured on the rough substrate with low-nanometer dimensions (Fig 10C). In addition, involvement of JNK in the regulation of ECJ development was further confirmed by showing that anisomycin, a pharmacological activator of JNK, disrupted the ECJs of the cell aggregates (Fig 10D). These results suggest that the delay in ECJ development may have been associated with JNK activity in the cells cultured on the rough substrate with low-nanometer dimensions. However, the responsiveness of ECJ development to JNK regulation was observed in HGKs cultured on the rough substrate with a low-nanometer dimension, but not in HGKs cultured on substrates with higher levels of roughness. There was no acceleration of ECJ development in response to JNK inhibition in the cells grown on substrates with higher levels of roughness (Fig 10B). These results indicate that the physical barrier of the very rough

substrates could not be overcome by the biological regulation of JNK activity when the cells were scattered at a low density. However, ECJ development in response to JNK inhibition in the cells grown on the substrates with greater levels of roughness was clearly upregulated when the cells were cultured at a high density to reduce the distance between cells. These results suggest that JNK inhibition can be used to promote ECJ development when oral keratinocytes are packed into the JE on rough surfaces with high-nanometer dimensions.

iv. DISCUSSION

The present study demonstrates that the formation of cell-to-cell junctions between human oral keratinocytes is regulated by cell signaling pathways. Therefore, the structural characteristics of the JE may be derived from differences in the signaling pathways controlling the intercellular junctions. The JE of mouse molars contained high JNK activity accompanied by poorly formed E-cadherin junctions. This inverse relationship between the development of the intercellular junctions and JNK activity were apparent *in vitro*. JNK activation downregulated E-cadherin expression at the site of the disrupted cellular junctions. These results strongly suggest that the poor development of intercellular E-cadherin junctions within the JE may be a result of high JNK activity. The dissociation of cell-to-cell junctions between oral keratinocytes may lead to a deterioration of the protective barrier provided by the oral epithelium against bacterial invasion or the diffusion of toxic substances, which ultimately leads to infection or inflammation of the connective tissue underlying the epithelium. It has been reported that E-cadherin expression decreases further within the pocket epithelium compared with the healthy JE [29]. These results indicate that JNK may be a master signaling molecule regulating the intercellular junctions within the JE. Furthermore, it is possible that JNK inhibition may prevent or treat gingivitis and periodontitis by promoting the strengthening of the intercellular junctions.

The JE is peculiar in that it has two basal laminae, one opposing the gingival connective tissue and the other opposing the solid enamel surface.

Interestingly, the JE interfaces with enamel, which is the stiffest surface in the human body. Thus, we hypothesized that the solid enamel surface may promote dissociation of E-cadherin junctions within the JE. To this end, we compared the cellular junctions between human oral keratinocytes cultured on stiff culture dishes to those formed on soft collagen gels. Dissociation of human oral keratinocytes from the culture dishes strongly points to the poor formation of intercellular E-cadherin junctions. Furthermore, this dissociation was associated with higher JNK and RhoA activities compared with the confluent layer of cells formed on the soft collagen gels. Based on these results, we conclude that the stiffness of a surface leads to the upregulation of RhoA, which in turn activates JNK, resulting in disruption of the intercellular junctions within the JE (Fig 9). The poor formation of adherens junctions between human skin keratinocytes grown on stiff surfaces further supports our hypothesis [43]. Studies using a conditional JNK or RhoA knockdown animal model will be required to confirm this hypothesis.

Also, we hypothesized that the solid and rough dentin surface can be affected to the junctional epithelial cells in case of which the periodontal pocket is getting deeper. Thus we compared the intercellular E-cadherin junctions with smooth and rough substrates. The development of E-cadherin junctions on rough substrate was defected and this disassembly of intercellular junction was affected by JNK activity. However, RhoA signaling on rough substrate is needed to be more investigated.

The finding that RhoA plays a role in regulating the intercellular junctions

between oral keratinocytes by activating JNK is notable because various bacterial toxins regulate RhoA activity. Therefore, it is likely that the E-cadherin junctions within the JE may be further destroyed if bacterial toxins also activate RhoA-JNK signaling. Although it is unknown whether oral bacteria regulate RhoA, it is well known that many bacteria secrete toxins that affect RhoA activity. CNF-1, used to activate RhoA in this study, is a 115-kDa toxin that is produced by uropathogenic *Escherichia coli* [44]. PMT, used to activate JNK (data not shown), is a 146-kDa toxin produced by *Pasteurella multocida*, the bacteria responsible for pasteurellosis, bite-wound dermonecrosis, and rhinitis in animals [45]. Exoenzyme C3, used in the present study to downregulate RhoA activity, is a 26-kDa molecule with ADP-ribosyltransferase activity that is produced by various bacteria including *Clostridium botulinum, Clostridium limosum, Staphylococcus aureus,* and *Bacillus cereus* [46].

In summary, the present study suggests that RhoA-JNK signaling may be associated with the structural defects of human oral keratinocyte intercellular junctions. However, inhibition of the RhoA-JNK signaling axis may ultimately be a way in which to strengthen these intercellular junctions. In fact, further study of this signaling axis may explain why the JE contains cells with wide intercellular junctions that are sparsely populated with E-cadherin and may suggest ways in which to strengthen the junctions to protect tooth-supporting gingiva from bacteria in the oral cavity.

v. FIGURES

Figure 1.

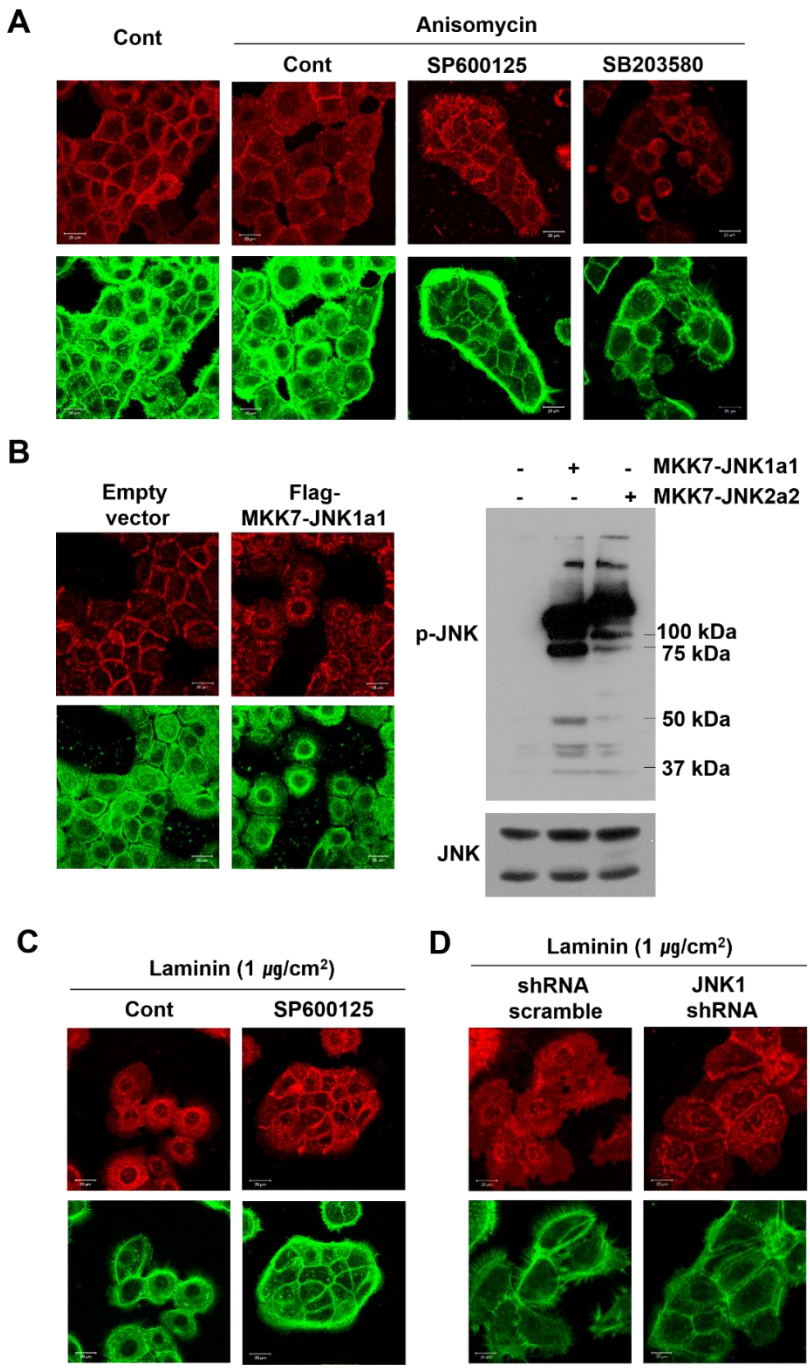

Figure 1. JNK regulates the formation of intercellular E-cadherin junctions between HOK-16B cells *in vitro*. The formation of E-cadherin junctions was determined by examining the expression level of E-cadherin (upper panels). F-actin was stained with FITC-phalloidin (lower panels). (A) Cells were treated with anisomycin, an activator of both JNK and p38 which had been pretreated with SB203580 (15 μM) or SP600125 (1 μM) to inhibit p38 activity or JNK activity respectively. Cells were cultured for 6 h. (B) Cells expressing constitutively active JNK1 were cultured for 2 days (left panel). Constitutive activation of exogenous JNK was confirmed by Western blotting (right panel). (C) Cells that grew in a scattered pattern on the laminin-coated hydrophobic dishes were treated with SP600125 (1 μM) for 24 h to inhibit JNK activity. (D) Cells infected with lentiviruses expressing shJNK to selectively inhibit JNK1 expression were cultured on laminin-coated hydrophobic dishes for 24 h. Scale bar, 20 μm.

Figure 2.

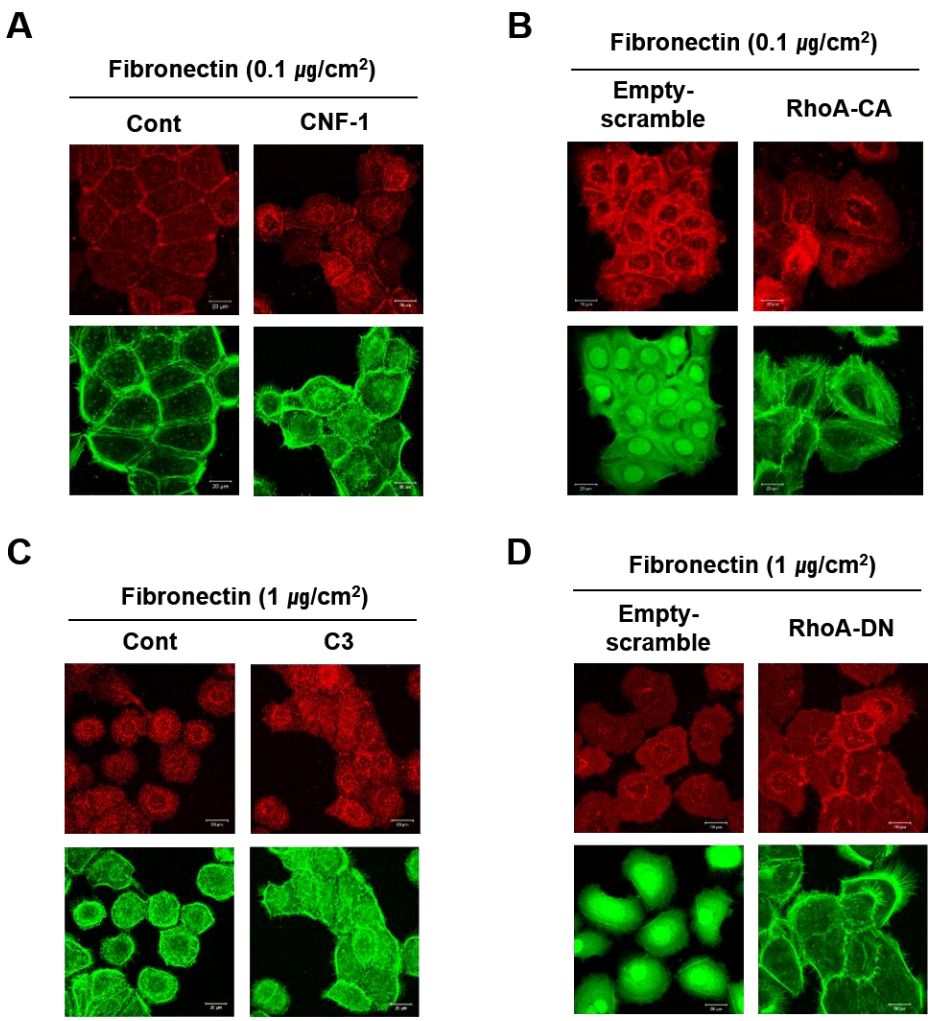

Figure 2. RhoA inhibits the formation of intercellular E-cadherin junctions between HOK-16B cells in vitro. The formation of E-cadherin junctions was determined by examining the expression level of E-cadherin (upper panel of each picture). F-actin was stained with FITC-phalloidin (lower panel of each picture). (A and B) The effect of RhoA activation on the

E-cadherin junctions was examined. Cells were cultured on fibronectin-coated plates containing 0.1 μg/cm2 fibronectin, which allowed cells to form intercellular junctions. RhoA activity was upregulated by treating cells with CNF-1 (0.5 μg/ml) for 24 h (A). Cells infected with lentiviruses expressing RhoA-CA were cultured for 24 h (B). (C and D) The effect of RhoA inactivation on the intercellular junctions was examined. Cells were cultured on fibronectin-coated plates containing 1 μg/cm2 fibronectin, which forced cells to grow in a scattered pattern without forming intercellular junctions. Cells were then treated with C3 for 6 h to inhibit RhoA activity (C). Cells infected with lentiviruses expressing RhoA-DN were cultured for 24 h (D). Scale bar, 20 μm.

Figure 3.

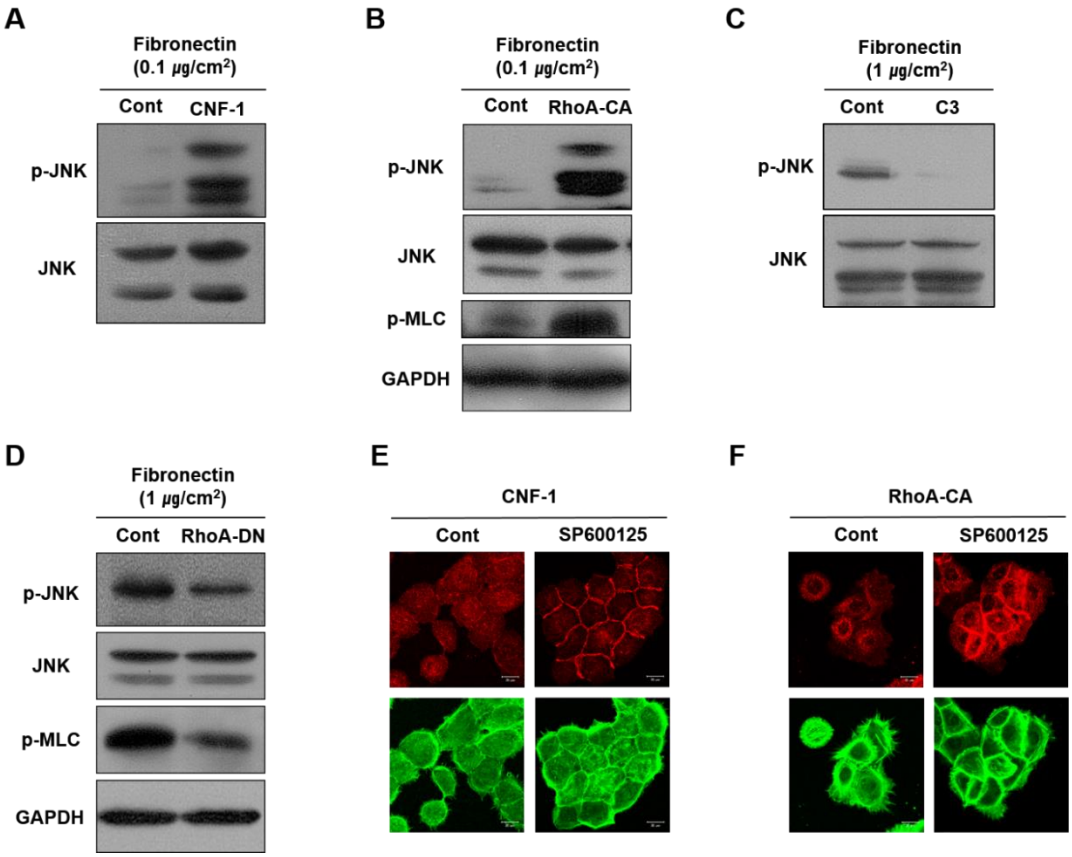

Figure 3. RhoA regulates the formation of intercellular E-cadherin junctions between HOK-16B cells by controlling JNK activity. (A - D) Regulation of JNK phosphorylation by RhoA was examined by Western blot analysis of cell lysates. p-MLC was also analyzed to confirm RhoA activity. Cells cultured on fibronectin-coated plates containing 0.1 μg/cm^2 fibronectin, which allowed cells to form intercellular junctions, were treated with the RhoA activator CNF-1 (0.5 μg/ml) for 24 h (A). Cells infected with lentiviruses

expressing RhoA-CA were cultured for 24 h. (C) Cells cultured on fibronectin-coated plates containing 1 μg/cm^2 fibronectin, which forced cells to grow in a scattered pattern without forming intercellular junctions, were treated with the RhoA inhibitor C3 (0.5 μg/ml) for 6 h. (D) Cells infected with lentiviruses expressing RhoA-DN were cultured for 24 h. (E-F) The formation of E-cadherin junctions was determined by examining the expression of E-cadherin (upper panels). F-actin was stained with FITC-phalloidin (lower panels). Cells pre-treated with SP600125 (1 μM) for 1 h or left untreated were additionally treated with the RhoA activator CNF-1 (1 μM) for 24 h to determine whether JNK was regulated by RhoA (E). Cells expressing RhoA-CA were seeded onto culture dishes and grown in the absence or presence of SP600125 (1 μM) for 12 h (F). Scale bar, 20 μm.

Figure 4.

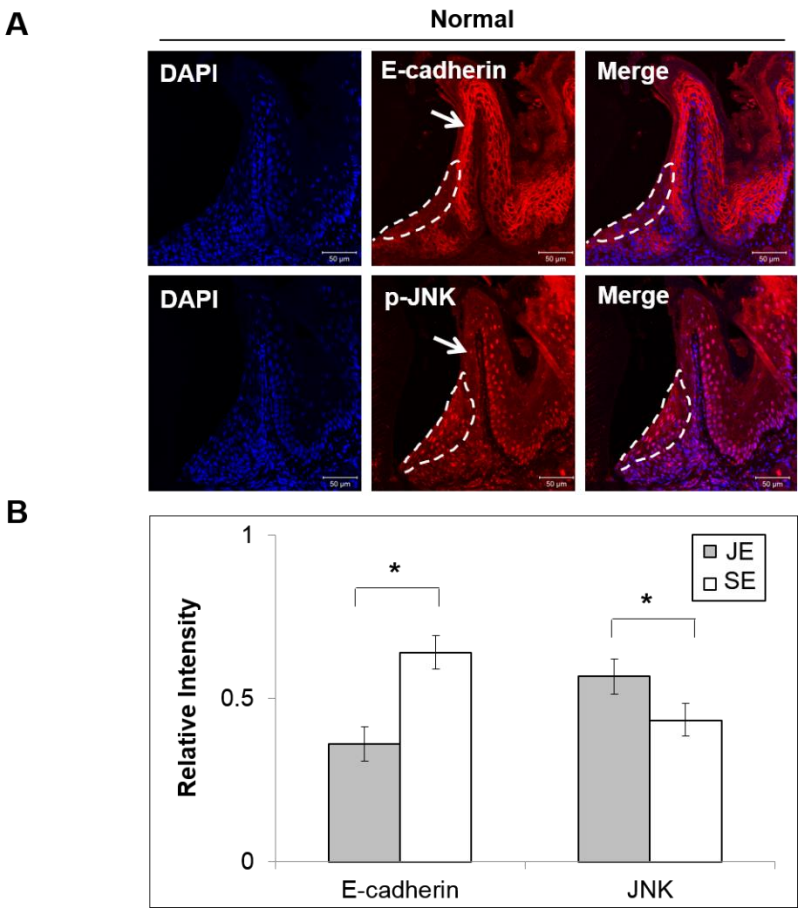

Figure 4. p-JNK is highly expressed within the intercellular junctions of the mouse junctional epithelium, whereas E-cadherin is poorly expressed. (A) Decalcified paraffin sections of mandibular molars, including surrounding tissue, were immunostained using antibodies against E-cadherin or p-JNK. Nuclei were stained with DAPI. In addition, E-cadherin expression levels following JNK inhibition were also examined. Dashed lines indicate the outline of the JE. Scale bar, 50 μm. (B) Relative intensity of the expression levels of E-cadherin and p-JNK within the JE and the GE were obtained by

dividing the intensity of the JE by the sum of the intensities of the JE and GE combined. Relative intensity of the GE was obtained by dividing the intensity of the GE by the sum of the intensities of the JE and GE. The data are expressed as the mean ± SD. n = 5. Each immunohistochemical datum was obtained from different mice. *, $p < 0.05$.

Figure 5.

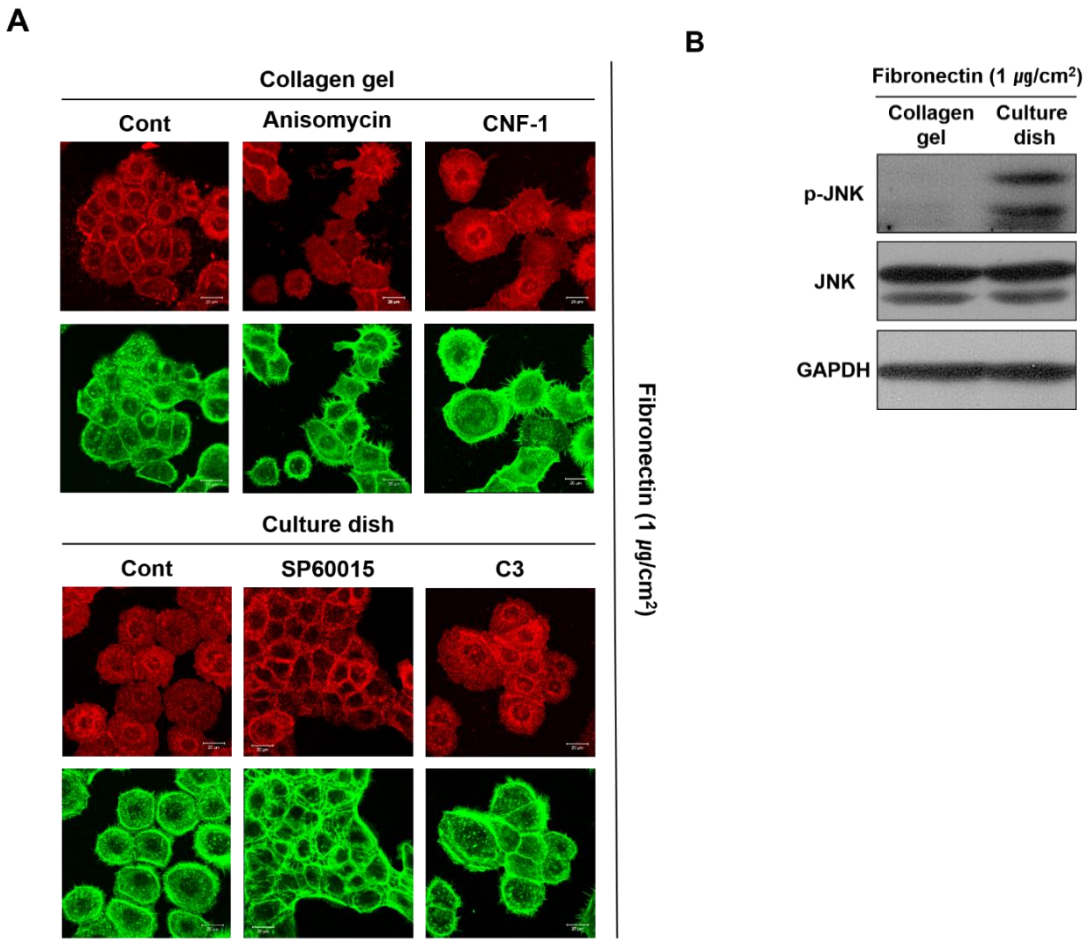

Figure 5. Intercellular E-cadherin junctions between HOK-16B cells are poorly formed due to the upregulation of p-JNK that results from growth on solid surfaces. (A) Cells were grown on polystyrene culture dishes or on soft collagen gels (coated with fibronectin, 1 μg/cm^2) for 24 h. Cells on the collagen gels were subsequently treated with anisomycin (1 μM) or CNF-1 (0.5 μg/ml) for 24 h to activate JNK or RhoA, respectively. Cells

on the culture dishes were subsequently treated with SP600125 (1 μM) or C3 (0.5 μg/ml) for 8 h to inhibit JNK or RhoA, respectively. Cells were examined by confocal laser microscopy after immunostaining for E-cadherin (upper panel) or after staining for actin filaments with FITC-phalloidin (lower panel). Stained cells were examined by confocal laser microscopy. Scale bar, 20 μm. (B) Cells were harvested by treating with dispase. Levels of JNK or p-JNK were analyzed by Western blotting.

Figure 6.

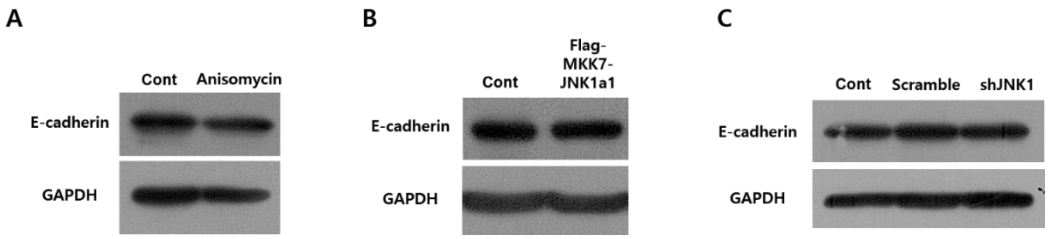

Figure 6. The expression level of E- cadherin was not changed by the regulation of JNK activity. (A, B, C) E-cadherin expression was analyzed by Western blotting after treating cells with anisomycin (1 μM) (A) or after transfection to express MKK7-JNK1a1 (B) or shJNK (C).

Figure 7.

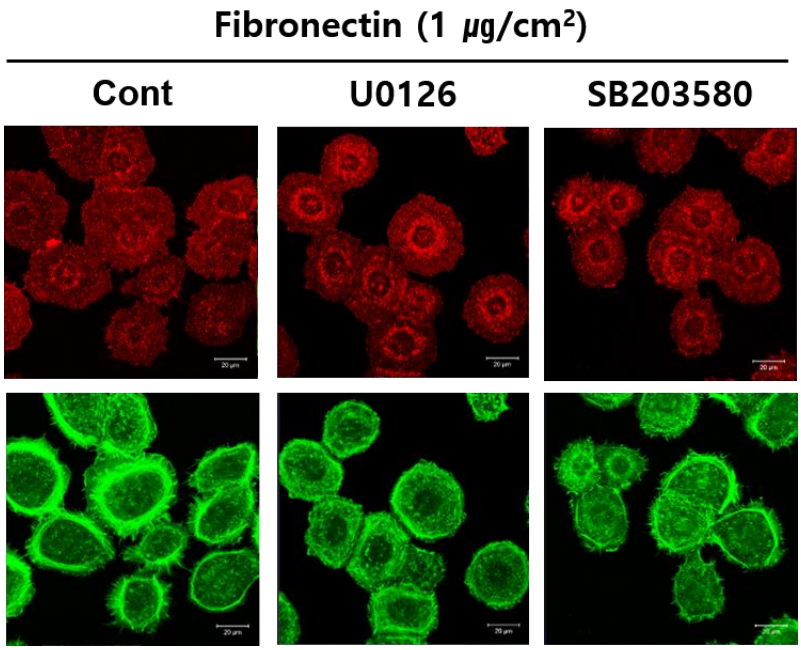

Figure 7. JNK, not ERK or p-38, regulates formation of intercellular E-cadherin junctions. Cells were cultured in the presence of U0126 (10 μM), an ERK inhibitor, or SB203580 (15 μM), a p38 inhibitor, on fibronectin-coated culture dishes (1 μg/cm^2 fibronectin) for 24 h. Scale bar, 20 μm.

Figure 8.

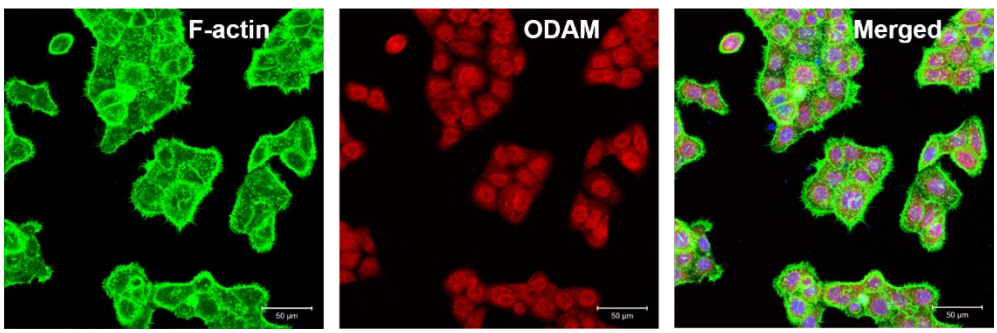

Figure 8. The localization and expression level of odontogenic ameloblast-associated protein precursor (ODAM) in HOK-16B. (A) Decalcified paraffin sections of mandibular molars, including surrounding tissue, were examined by light microscopy (LM) or transmission electron microscopy (TEM) after HE or uranium/lead staining, respectively. ES indicates the empty space that appeared after complete decalcification of the enamel matrix. (B) TEM magnified the junctional epithelium (JE) and gingival epithelium (GE) shown as a box in Fig A. The upper part of the JE is surrounded by the GE in mice. Intercellular junctions within the JE were loosely formed, whereas intercellular junctions within the GE were tightly formed. Arrows indicate the intercellular spaces between the cells of the JE. * indicates the artificially separated gap between the JE and the GE. (C) ODAM (arrow) is strongly expressed in the JE but not in the GE of mice.

Immunohistochemical staining of ODAM was performed to differentiate the JE from the GE. Decalcified sections of mandibular molars, including surrounding tissue, were immunostained using antibodies raised against ODAM. Nuclei were stained with DAPI. ES: enamel space, D: dentin, CT: connective tissue. Scale bar, 50 μm.

Figure 9.

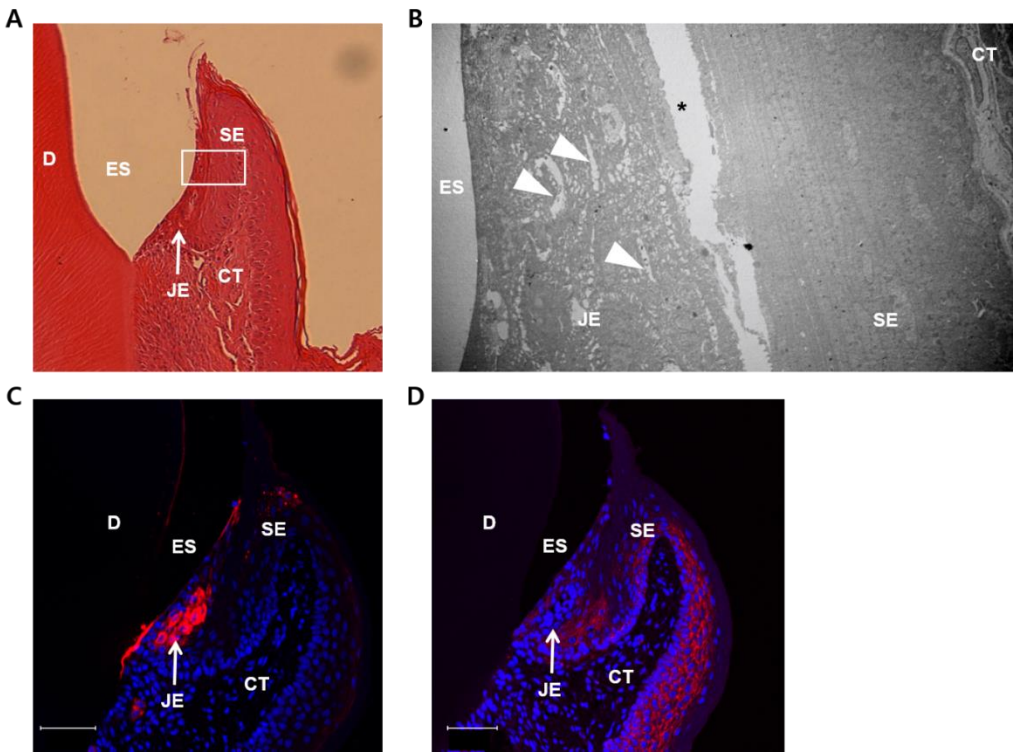

Figure 9. Diagram of a hypothetical molecular mechanism in which cell attachment to a solid enamel surface leads to poorly formed intercellular junctions within the JE. JNK activated by RhoA, a result of cell attachment to solid surfaces such as enamel, may inhibit the development of E-cadherin junctions within the JE. In addition, this hypothetical mechanism suggests a possible role for bacteria in the regulation of these intercellular junctions through the modulation of RhoA activity. Furthermore, regulation of RhoA and/or JNK may provide a novel way in which to regulate the barrier structure

of the JE to prevent or treat periodontitis.

Figure 10.

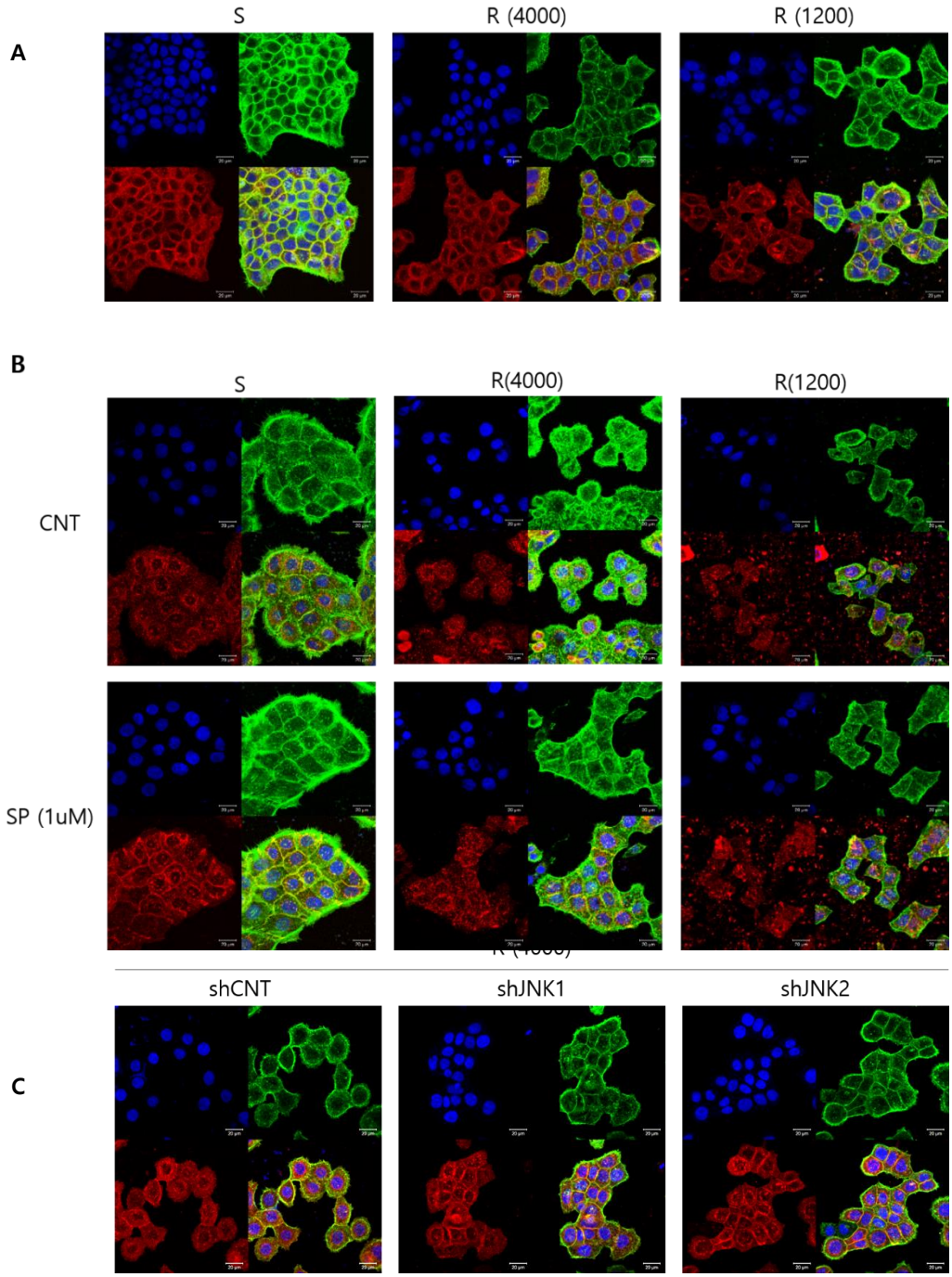

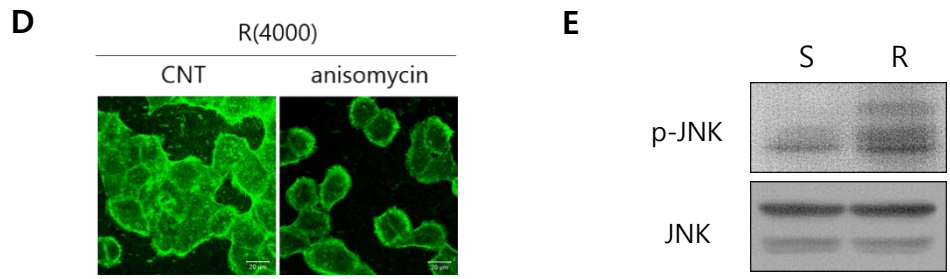

Figure 10. Influence of JNK on ECJ development on rough surface. (A) HGKs were cultured on substrates with varying levels of roughness. The images were measured by immunocytochemical staining for the expression level of E-cadherin (red). F-actin (green) was stained with FITC-phalloidin. Nuclei were stained with DAPI (blue). The lower right picture in each set of 4 pictures is a merged image of the E-cadherin, F-actin, and nuclei images. (B) HGKs were treated with SP (1 μM) to inhibit JNK activity for 24 hours in culture starting 12 hours after cell seeding on the smooth and rough substrates. CNT indicates the control culture without treatments with SP. (C) HGKs transfected using lentiviruses expressing shJNK1/2 to selectively inhibit JNK1/2 activity were re-plated for 24 hours on the rough substrate with low-nanometer dimensions (Ra=121.3±13.4 nm). ECJ development was followed by immunocytochemical staining for the expression level of E-cadherin (red). F-actin (green) was stained with FITC-phalloidin. Nuclei were stained with DAPI (blue). The lower right picture in each set of 4 pictures is a merged image of the E-cadherin, F-actin, and nuclei images. shCNT, scrambled shRNA. (D) HGKs were treated with anisomycin (20 ng/mL) to activate JNK

for 20 hours in culture starting 3 days after cell seeding on the rough substrates. CNT indicates the control culture without treatments with anisomycin (bar=20 μm). Ra=121.3±13.4, 505.3±115.3, and 867.0±168.6 nm for R(4000), R(1200), and R(200), respectively. (E) Immunoblot assay was conducted in HGKs cultured on smooth(S) or rough (R: R#4000) for 24h.

S: smooth substrate, SP: SP600125, JNK: c-Jun N-terminal kinase, ECJ: E-cadherin junction, HGK: human gingival keratinocyte, CNT: carbon nanotube, Ra: average roughness, p-JNK: phospho-c-Jun N-terminal kinase, shRNA: small hairpin RNA, FITC: fluorescein isothiocyanate-labeled, DAPI: 4', 6-diamidino-2-phenylindole dihydrochloride, R(4000): prepared with #4000 sandpaper, R(1200): prepared with #1200 sandpaper, R(200): prepared with #200 sandpaper.

Chapter Ⅲ

Inherently up-regulated JNK activity dissociates YD-10B oral squamous carcinoma cells

* This chapter has been largely reproduced from an article published by Lee, G.Y. and Kim H.M. (2017) Biochemical and Biophysical Research Communications, 487(4):862-867.

i. INTRODUCTION

The development of intercellular junctions is one of the most unique characteristics of epithelial cells. The destruction of intercellular junctions, an event that occurs in the epithelial-mesenchymal transition (EMT), results in the metastasis of epithelial cancer cells. Thus, the molecular mechanism by which the development of intercellular E-cadherin junction (ECJs) between epithelial cells is regulated has been intensely investigated. C-Jun N-terminal kinases (JNKs) regulate many physiological or pathological processes such as various stresses, inflammation, cell proliferation, differentiation, morphogenesis, cell migration, survival and death [47, 48]. Recently, it has been reported that JNKs are associated with the dissociation of epithelial cells. High JNK activity persistently induced by pharmacological drugs or constitutively induced by transfecting MKK4/7-JNK1/2 inhibits the development of ECJs between normal human skin keratinocytes [35]. The authors also reported that the development of ECJs of normal human oral keratinocytes is suppressed when JNK activity is constitutively up-regulated [49]. JNK mediates the disassembly of intestinal epithelia at apical junctions [50]. In addition, the metastasis of pancreatic cancer cells is promoted on type I collagen substrates through the up-regulation of JNK activity [51]. These previous reports suggest that epithelial carcinoma cells may grow scattered if their JNK activity is inherently up-regulated.

YD-10B cells, which are established from human oral squamous carcinoma

cells developed in the male tongue, grow scattered without the development of ECJs, although they express epithelial markers such as E-cadherin and do not express mesenchymal markers such as vimentin [52]. The present study investigated whether JNK was associated with the scattered growth through suppressing the development of ECJs in these oral squamous carcinoma cells that maintained the molecular epithelial phenotype. The results of the present study may improve our understanding of the molecular mechanism by which epithelial carcinoma cells disassemble ECJs to dissipate, an event that occurs in the early phase of tumorigenesis.

ii. MATERIALS AND METHODS

1. Reagents and materials

Antibodies for E-cadherin, c-Jun N-terminal kinase (JNK), phospho-c-Jun N-terminal kinase (p-JNK: Thr183/Tyr185), glyceraldehyde 3-phosphate dehydrogenase (GAPDH), and horseradish peroxidase (HRP)-linked anti-rabbit IgG were purchased from Cell Signaling Technology (Waltham, MA, USA). Cy3-conjugated anti-rabbit IgG antibody was obtained from Jackson ImmunoResearch (West Grove, PA). Fluorescein isothiocyanate-labeled phalloidin (FITC-phalloidin), 4′,6-diamidino-2-phenylindole dihydrochloride (DAPI), SP600125 (JNK inhibitor), anisomycin (JNK activator), and puromycin were obtained from Sigma-Aldrich (St. Louis, MO, USA). pcDNA3 Flag MKK7B2Jnk1a1 (constitutively active JNK1) and pCDNA3 Flag MKK7B2Jnk2a2 (constitutively active JNK2) were gifts from Roger Davis (Addgene plasmid # 19726, # 19727 respectively, Cambridge, MA) [53]. pCSCG was a gift from Inder Verma (Addgene plasmid # 12154) [54]. pCS-CG-MKK7B2Jnk1a1 and pCSCG-MKK7B2Jnk2a2 were generated by Cosmo Genetech (Seoul, Korea). The plasmids of JNK1/2 shRNA (shJNK1/2) were purchased from Santa Cruz Biotechnology (Santa Cruz, CA). psPAX2 was a gift from Didier Trono (Addgene plasmid # 12260). pMD2.G was a gift from Didier Trono (Addgene plasmid # 12259). Lipofectamine LTX and Plus reagents were obtained from Invitrogen (Carlsbad,

CA). Transwell cluster plates (6.6 mm; 8.0-μm pore size) were purchased from Costar (Cambridge, MA).

2. Cell culture and transfection

YD-10B and YD-8 cells, cell lines established from the biopsies of human oral squamous carcinoma cells, were obtained from SNU cell banks [52]. YD-10B and YD-8 cells were cultured in RPMI1640 (WELGENE, Gyeongsan-si, Korea). SCC-25 human squamous carcinoma cells were obtained from ATCC (Manassas, VA). SCC-25 cells were cultured in DMEM/F12 (WELGENE, Gyeongsan-si, Korea). HOK-16B cells, which are immortalized cells from periodontally healthy human retromolar gingival tissue, were a gift from Dr. N.-H. Park (School of Dentistry, University of California, Los Angeles, USA) [55]. HOK-16B cells were cultured in KGM keratinocyte growth medium supplemented with bovine pituitary extract, GA-1000 (gentamicin, amphotericin-B), hydrocortisone, rhEGF, insulin (recombinant human) (Lonza, Basel, Switzerland), and 1% penicillin. Cell transfection was performed as described previously [49]. Briefly, HEK 293T cells were transfected with pCS-CG-MKK7b2-JNK1a1, pCS-CG-MKK7b2-JNK2a2, or plasmids JNK1/2 shRNA (shJNK1/2), together with pMD2.G and psPAX2 to produce lentiviral particles using Lipofectamine LTX and Plus reagents. Next, the viral supernatants of HEK 293T cells were used to infect YD-10B cells. Cells were

selected by puromycin. Transfected cells expressed the green fluorescence protein (GFP) with varying intensities.

3. Immunoblotting

Immunoblotting was performed according to the standard protocol. Briefly, the cells were lysed with a lysis buffer (150 mM NaCl, 1% deoxycholate, 20 mM Tris-HCl (pH 7.5), 1 mM EDTA, 1% Triton X-100, 1 mM EGTA, 2.5 mM sodium pyrophosphate, 1 mM glycerophosphate) containing a protease inhibitor mixture consisting of 1 mM Na3VO4, 10 mM NaF, and 1 mM PMSF protease inhibitor (Boehringer, Mannheim, Indianapolis), 1 μg/ml leupeptin, and 1 μg/ml aprotinin phosphatase inhibitors (Calbiochem, La Jolla, CA). Cell lysates boiled in sample buffer were sizeseparated via SDS-PAGE and were transferred to polyvinylidene difluoride membranes. The membranes blocked with 5% skim milk were incubated with primary antibodies overnight at 4° C. Next, the membranes were incubated with secondary antibodies in 5% skim milk for 1 hr at room temperature. The blots were developed using enhanced chemiluminescent horseradish peroxidase substrate (Invitrogen, Carlsbad, CA).

4. Immunocytochemistry

Immunocytochemistry was performed according to the standard protocol. Briefly, cells were fixed with 4% v/v paraformaldehyde and were permeabilized in 0.5% v/v Triton X-100. The cells were incubated with primary antibody raised against E-cadherin at RT for 2 hrs. Next, the cells were treated with Cy3-conjugated anti-rabbit IgG antibody. F-actin was stained with FITC-phalloidin. Nuclei were stained with DAPI. Images of the stained cells were obtained using an LSM 700 confocal laser-scanning microscope (Zeiss, Oberkochen, Germany). In addition, images of Ecadherin and F-actin were merged to co-localize E-cadherin and F-actin. Quantitative data for the development of ECJ were obtained by dividing the total length of ECJ with the number of cells found in a picture taken by LSCM. Images were measured using ImageJ (NIH, Bethesda, MD.

5. Migration assay

Narrow scratches were made across the confluently grown cells using micropipette tips. Because YD-10B cells migrated highly rapidly, cell migration for 6 hrs was analyzed. Empty areas devoid of cells in the fixed area were measured using ImageJ on the images obtained by phase contrast microscopy because the migration front was not straight. The areas devoid of cells at 0 or 6 hrs were used to calculate the relative migration rates. Uniquely, the borders of the initially scratched areas were not discernible for YD-10B cells because they rapidly grew to mask the border line of the initial wounds

at 0 hrs. Thus, the average area free of cells at 0 hrs was used as an area at 0 hrs in the calculation of the migration rates. The migration rate was calculated as follows: Migration rate = (average area free of cells at 0 hrs − area devoid of cells at 6 hrs) / average area free of cells at 0 hrs.

6. Statistical analysis

Statistical analyses were performed using MedCalc version 17.2 for Windows (MedCalc software, Ostend, Belgium). Statistical analyses were performed to compare the two groups using independent samples t−test when the data were in normal distribution or the Mann−Whitney test when the data were not in normal distribution. To compare more than two groups, one−way analysis of variance was used when the data were in normal distribution, and the Kruskal−Wallis test was used when the data were not in normal distribution. Post hoc tests for pairwise comparisons were analyzed using the Tukey−Kramer test after one−way analysis of variance and the Mann−Whitney test after the Kruskal−Wallis test. A P−value <0.05 was considered statistically significant.

iii. RESURLTS AND DISCUSSION

YD-10B cells expressed a high level of epithelial markers such as E-cadherin as normal oral keratinocytes, HOK-16B cells, and did not express mesenchymal markers such as vimentin and N-cadherin, which were expressed in other squamous carcinoma cells such as SCC25 and YD-8 cells (Fig 11A) [56-60]. This epithelial phenotype of YD-10B cells devoid of mesenchymal markers suggests that they are at the early phase of transformation. Unexpectedly, however, YD-10B cells grew scattered without the development of ECJs on substrates used for cell culture and showed a high migration rate as other mesenchymal squamous carcinoma cells, such YD-8 cells (Fig 11B). The scattering of YD-10B cells was confirmed on the substrates that were pre-coated with a definite amount of fibronectin on the hydrophobic dishes (Fig 11C). YD-10B cells scattered on the substrates where HOK-16B normal keratinocytes or SCC-25 epithelial tumor cells aggregated. The scattered growth of YD-10B cells was remarkable in that they definitely maintained the epithelial phenotype and did not express mesenchymal markers. We noticed that the expression level of p- JNK was up-regulated in YD-10B cells compared to epithelial HOK-16B or SCC-25 cells (Fig 1A). JNK has been reported to be associated with the development of E-cadherin junctions in normal or tumor epithelial cells [35, 50, 51]. JNK activity is associated with the development of ECJs in normal human skin keratinocytes. In addition, apical junctions are disassembled by activating JNK

in intestinal epithelia. Some tumor cells dissociate on the collagen matrix through the up-regulation of JNK activity. Recently, we reported that JNK activity is detrimental to the development of ECJs in normal human oral keratinocytes [49]. Thus up-regulated expression of p-JNK was further investigated whether it was associated with the scattering of YD-10B cells.

The up-regulated JNK activity of YD-10B cells was suppressed to examine whether downregulated

JNK activity reversed the scattered growth of the cells through inducing the development of ECJs. Lowered JNK activity, by treating cells with SP600125, a pharmacological JNK inhibitor, aggregated cells with the development of ECJs (Fig 12A). Knock-down of JNK1/2, by transfecting the cells with shJNK1/2 lentiviral supernatant produced in HEK 293T cells, also induced the development of ECJs in YD-10B cells (Fig 12B). These results indicate that YD-10B cells grow scattered due to the inherently up-regulated JNK activity. It is interesting that carcinoma cells dissociate due to the change in a single modality, JNK activity, despite the high expression of E-cadherin. Furthermore, inhibiting JNK activity significantly suppressed cell migration, which is critical in the dissipation of cancer cells (Fig 12C). Cohesive growth of the tumor cells following the development of E-cadherin junctions may slow down the outward migration of the tumor cells. Interestingly, the p-JNK level of YD-10B cells varied depending on the adhesion strength of the cells to the substrates (Fig 13A). According to the decreasing amount of pre-coated

fibronectin before cell seeding, the expression of p-JNK was tentatively decreased concomitant with the interim decrease in cell scattering along with the increase in the development of E-cadherin junctions, although the cells momentarily scattered after culture for 2 days. In addition, the expression level of p-JNK was remarkably low, and E-cadherin junctions were obviously developed in the cells cultured at high density, allowing unconstrained physical cell contacts (Fig 13B). These results indicate that E-cadherin of YD-10B cells is functionally intact and, more importantly, confirm that the expression level of p-JNK is associated with the development of E-cadherin junctions in YD-10B cells. However, it was uncertain whether cell contacts lowered the expression of p-JNK or the lowered expression of p-JNK promoted the development of E-cadherin junctions. To solve this issue, YD-10B cells in which JNK activity was consistently up-regulated using anisomycin, a pharmacological JNK activator, or was constitutively activated by transfecting MKK7-JNK1/2, were examined to determine whether JNK activity inhibited the development of E-cadherin junctions or destroyed the pre-developed E-cadherin junctions in cultures on substrates pre-coated with a low amount of fibronectin or cultures at a high density to force physical contacts. YD-10B cells in which JNK activity was persistently or constitutively activated apparently did not develop E-cadherin junctions despite the culture conditions inducing the development of E-cadherin junctions to our suggestions (Figs 14A - C). The E-cadherin junctions of YD-10B cells that were cultured at confluency did not develop when JNK was constitutively activated by

expressing the MKK7-JNK1/2 fusion protein using lentiviral vectors (Fig 14A). E-cadherin junctions that had developed by culturing the cells to confluence were disassembled to create intercellular gaps by pharmacological JNK activation with anisomycin treatment (Fig 14B). In addition, E-cadherin junctions developed on substrates pre-coated with a low amount of fibronectin were also destroyed to generate intercellular gaps by persistent JNK activation with anisomycin treatment (Fig 14C). These results further confirm that YD-10B cells grow scattered due to the high JNK activity, although they maintain the epithelial phenotype, such as the expression of functional E-cadherin. The involvement of inherent JNK activity in the destruction of the cell-cell junctions in epithelial carcinoma cells demonstrated in the present study has not been reported to our limited knowledge, although inherently activated JNK is associated with other events related to tumorigenesis in some cancer cells. The role of hepatocellular carcinoma cells or prostate cancer cells that are high in the activity or expression level of JNK has been reported to be associated with events other than the dissociation of the cell-cell junction [61-65].

Next, we noticed the up-regulated expression of p-JNK in YD-10B cells compared to HOK-16B cells or SCC-25 cells on the same substrates where YD-10B cells scattered but HOK-16B cells or SCC-25 aggregated (Fig 11). These findings propose a possibility that the pathway activating JNK depending on adhesion signaling to the substrates may be associated with the dissociation of the ECJs in YD-10B cells (Fig 13A). If this is the case,

extraordinarily up-regulated p-JNK may dissociate and dissipate YD-10B cells through the matrix of tissues which does not induce the scattering of other carcinoma cells such as SCC-25 cells in which JNK activation is less responsive to adhesion signaling. Further study regarding the signaling pathway associated with the hyper responsiveness of squamous carcinoma cells to adhesion signaling in the activation of JNK may improve our understanding of the molecular mechanism by which epithelial carcinoma cells disassemble the E-cadherin junctions to dissipate, an event that occurs in the early phase of tumorigenesis. In summary, the present study demonstrated that YD-10B cells lose epithelial cohesiveness due to the inherently up-regulated JNK activity, despite their high expression of functional E-cadherin, which is the pre-requisite for the transformation of the epithelial tumor cells to mesenchymal cancer cells. The present study also shows that the suppression of JNK activity restores their epithelial growth through developing E-cadherin junctions. However, further study is required to investigate what inherently up-regulates JNK activity at the early stage of the tumorigenic process while they highly express functional E-cadherin. Oral squamous carcinoma-derived YD-10B cells may be a model cell line for such studies due to its unique and high responsiveness of JNK to adhesion strength.

iv. FIGURES

Figure 11.

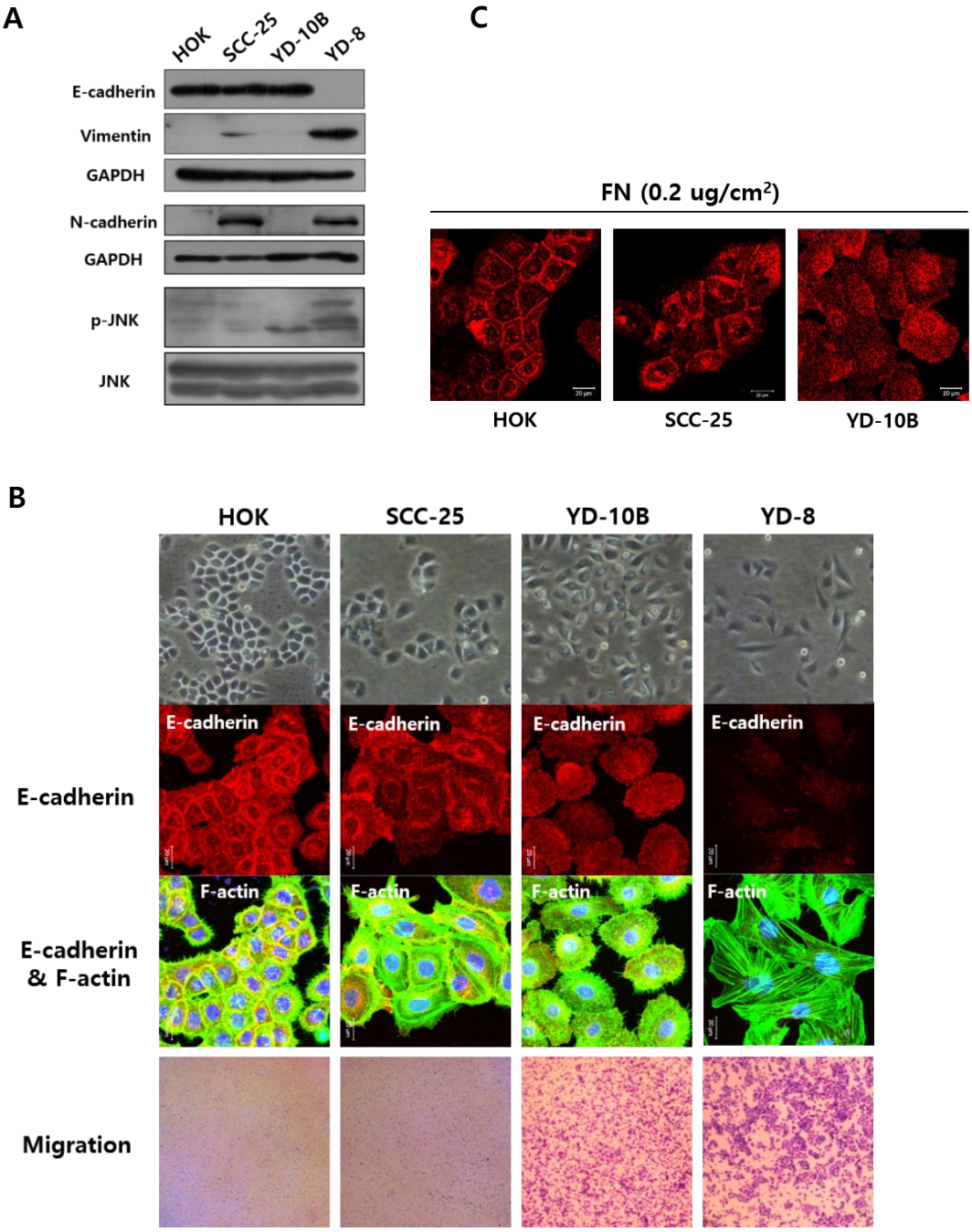

Figure 11. Phenotypes of the HOK-16B normal human oral keratinocyte cell line and various squamous cell carcinoma cell lines (SCC25, YD-10B, YD-8) derived from oral keratinocytes. (A) Various cells were cultured routinely in cell culture dishes for 24 hrs. Next, the expression levels of E-cadherin, vimentin, N-cadherin, and p-JNK were compared by immunoblotting methods. (B) Various cells were cultured routinely on cell culture dishes for 24 hrs. The cells were then observed by phase contrast microscopy or CLSM after staining E-cadherin (Red) by immunocytochemical methods or staining F-actin (Green) with FITC-phalloidin. Merged images of E-cadherin and F-actin were over-exposed to co-localize them. Nuclei were stained with DAPI. Cell migration was assayed using transwell cluster plates. Cells placed on the upper surface of the filter in chambers were incubated at 37° C for 24 hrs. Next, the cells migrated through the filter were recorded after staining. Original magnification of phase contrast microscopic images: ×100. (C) Various cells were cultured on hydrophobic dishes that were pre-coated with fibronectin (0.2 μg/cm2) for 24 hrs. Next, the cells were observed by CLSM after staining E-cadherin (Red) by immunocytochemical methods. Scale bar: 20 μm.

Figure 12.

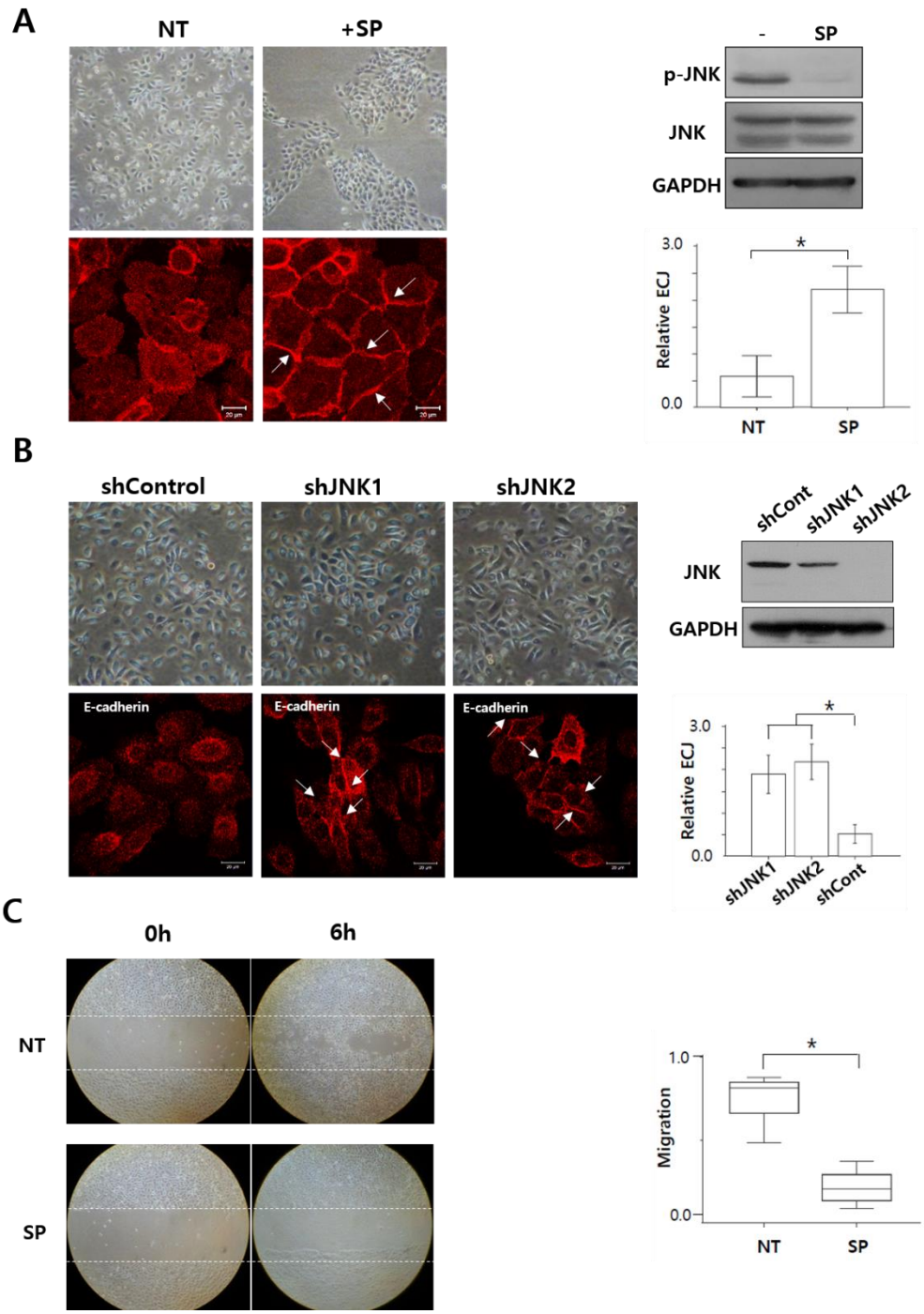
A
NT
+SP
- SP
p-JNK
JNK
GAPDH
3.0
0.0
Relative ECJ
*
NT
SP
B
shControl
shJNK1
shJNK2
shCont
shJNK1
shJNK2
JNK
GAPDH
E-cadherin
E-cadherin
E-cadherin
3.0
0.0
Relative ECJ
*
shJNK1
shJNK2
shCont
C
0h
6h
NT
SP
1.0
0.0
Migration
*
NT
SP

Figure 12. Effects of lowered JNK activity on E-cadherin junctions and cell migration of YD-10B cells. (A) YD-10B cells cultured for 18 hrs were further cultured routinely in cell culture dishes with SP600125 (SP) (5 μM) for 20 hrs to suppress the activity of JNK. Next, cells were observed by phase contrast microscopy or CLSM after staining E-cadherin (Red) by immunocytochemical methods. A lowered expression level of p-JNK by SP treatments was confirmed by immunoblotting methods. Statistical analysis was performed using independent sample t-test because the data were in normal distribution. Bar plot (mean ± SD). *$p < 0.05$, n = 3 and 4 for NT and SP, respectively. NT: control culture without SP600125. Arrows: E-cadherin. Scale bar: 20 μm. Original magnification of phase contrast microscopic images: ×100. (B) YD-10B cells were transfected with the supernatant of HEK 293T cell cultures producing lentiviral particles containing JNK shRNA for 2 days. Next, cells were selected by puromycin and replated on the cell culture dishes. Transfected cells were observed by phase contrast microscopy or CLSM after staining E-cadherin (Red) by immunocytochemical methods after culture for 24 hrs. A lowered expression level of p-JNK by transfecting shJNK was confirmed by immunoblotting methods. Statistical analysis was performed using one-way analysis of variance followed by post hoc analysis of the Tukey-Kramer test for pairwise comparisons because the data were in normal distribution. Bar plot (mean ± SD). *$p < 0.05$ (n = 2, 2, and 3 for shCont, shJNK1, and shJNK2, respectively). shCont: scramble shRNA. Arrows: E-cadherin. Scale bar: 20 m. Original magnification of phase contrast

microscopic images: × 100. (C) YD-10B cells were cultured to confluency for 48 hrs. Next, the cells were treated with SP (5 μM) for 6 hrs after scratching to detach the cells from the culture surfaces. The migration rates were assessed by the methods described in the Materials and Methods section. Statistical analysis was performed using non-parametric Mann-Whitney test because the data were not in normal distribution. Box-and-Whisker plot (the centerline: median). *P < 0.05, n = 15 and 16 for CNT and SP respectively. NT: control culture without SP600125.

Figure 13.

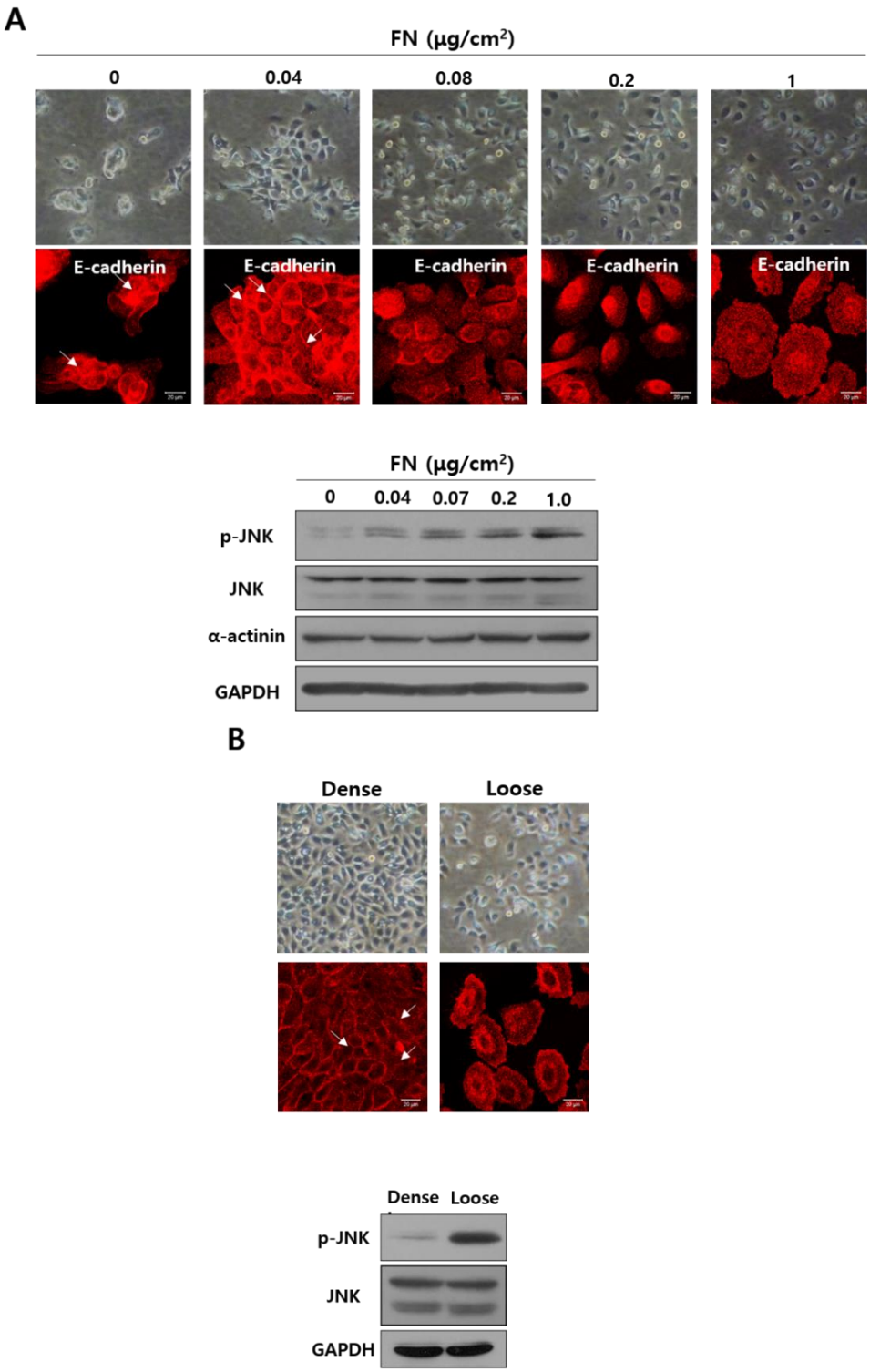
A
FN (μg/cm²)
0
0.04
0.08
0.2
1
E-cadherin
E-cadherin
E-cadherin
E-cadherin
E-cadherin
FN (μg/cm²)
0
0.04
0.07
0.2
1.0
p-JNK
JNK
α-actinin
GAPDH
B
Dense
Loose
Dense
Loose
p-JNK
JNK
GAPDH

Figure 13. Effects of the culture conditions of YD-10B cells with varying adhesion strengths to the substrates or cell density on the development of E-cadherin junctions. (A) YD-10B cells were cultured on hydrophobic culture dishes pre-coated with varying amounts of fibronectin (FN) for 24 hrs. Fibronectin was pre-coated on hydrophobic polystyrene dishes at 37° C for 2 hrs. The dishes were then blocked with 5% BSA for 1 hr at 37° C. (B) YD-10B cells were cultured routinely in cell culture dishes at low confluency (loose) or at confluency to induce physical contact (dense) for 24 hrs. (A - *B*) Cells were observed using phase contrast microscopy (upper lane) or CLSM (mid lane) after staining E-cadherin (Red) by immunocytochemical methods. The expressions levels of p-JNK in YD-10B cells were examined by immunoblotting methods after cell culture for 24 hrs, respectively. Arrows: E-cadherin. Scale bar: 20 μm. Original magnification of phase contrast microscopic images: ×100.

Figure 14.

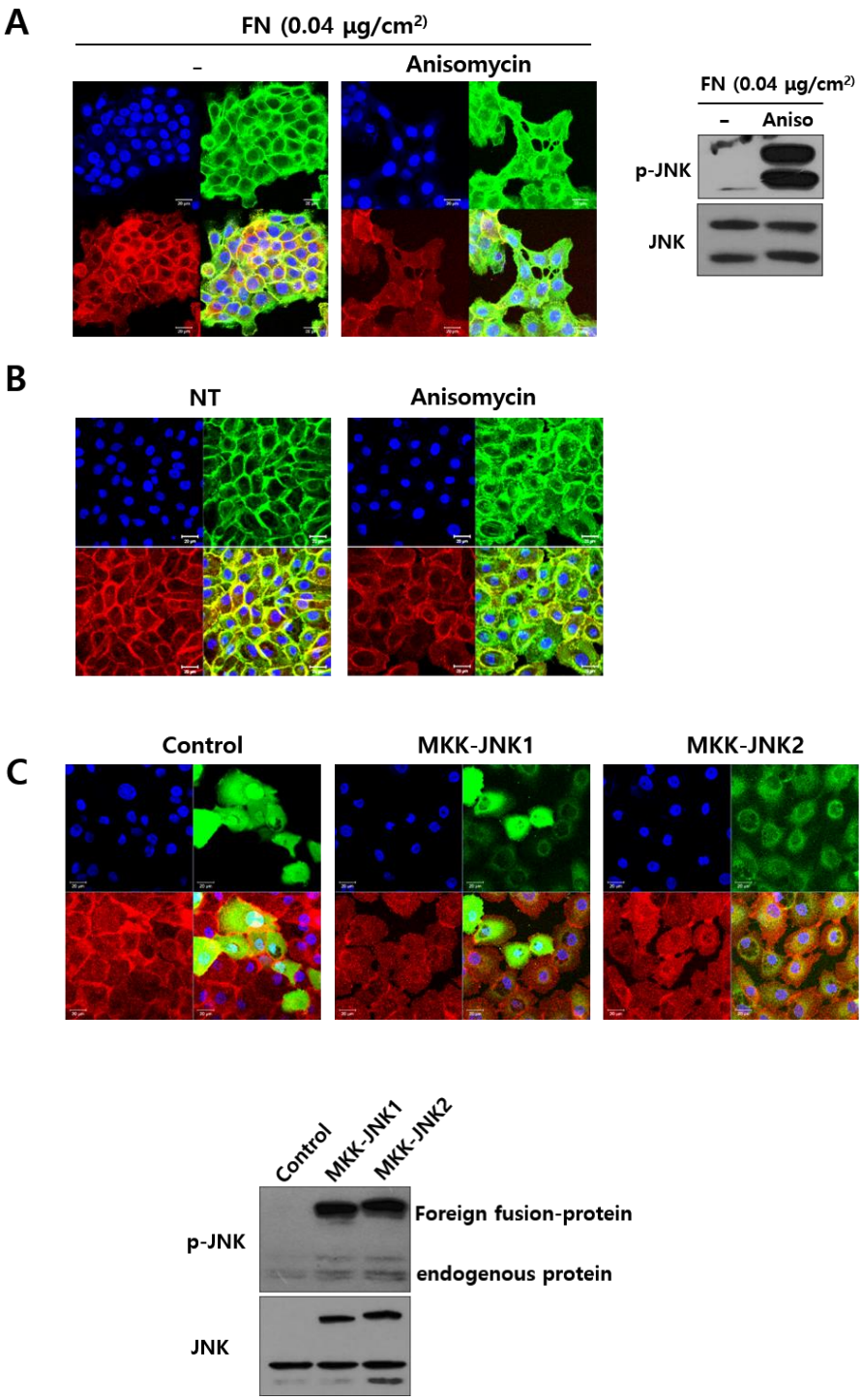
A
FN (0.04 μg/cm2)
–
Anisomycin
FN (0.04 μg/cm2)
–
Aniso
p-JNK
JNK
B
NT
Anisomycin
C
Control
MKK-JNK1
MKK-JNK2
Control
MKK-JNK1
MKK-JNK2
p-JNK
Foreign fusion-protein
endogenous protein
JNK

Figure 14. Effect of the constitutive JNK activation on the development of E-cadherin junctions in YD-10B cells. (A) YD-10B cells in which JNK expression was constitutively activated by the supernatant of HEK 293T cell cultures producing lentiviral particles containing plasmid for MKK7-JNK1/2 expression were selected with puromycin for 2 days. Next, the selected cells were cultured routinely for 3 days in cell culture dishes to confluency to induce the development of E-cadherin junctions. Control (NT) dishes were incubated with the supernatant of HEK 293T cell cultures producing lentiviral particles devoid of plasma for MKK7-JNK1/2 expression. Cells were observed by CLSM after staining E-cadherin (Red) by immunocytochemical methods and nuclei (blue) with DAPI. Green: Exogenous GFP. Pictures at the bottom right are the merged images of E-cadherin, exogenous GFP, and nucleus. The expression levels of p-JNK (fusion proteins and endogenous proteins) were confirmed by immunoblotting p-JNK. (B) YD-10B cells were treated with anisomycin (50 ng/ml) to disrupt E-cadherin junctions through activating JNK for 16 hrs when cells reached confluence on cell culture dishes for 24 hrs. Intercellular gaps (arrows). (C) YD-10B cells were treated with anisomycin (50 ng/ml) for 24 hrs to disassemble the E-cadherin junctions through activating JNK for the cells cultured on the substrates pre-coated with a low amount of FN (0.04 μg/cm2) for 20 hrs. The increased level of expression of p-JNK by treating cells with anisomycin was confirmed by immunoblotting p-JNK. Intercellular gaps (arrows). (B - C) Cells were observed by CLSM after staining E-cadherin (Red) by immunocytochemical methods or staining F-

actin (Green) with FITC-phalloidin. The pictures at the bottom right are merged images of E-cadherin, Factin, and nucleus. NT: control. Scale bar: 20 μm.

CHAPTER Ⅳ

CONCLUDING REMARKS

From the results of the present study, it is indicated that the decreased formation of intercellular E-cadherin junctions between human gingival keratinocytes may be coupled to high RhoA-JNK activity. The present study also clearly demonstrates that JNK activity is closely associated with adhesion condition of oral keratinocytes to the substrates such as substrate pliability, substrate roughness, and adhesion strength. In addition, JNK characteristically over-stimulated on the substrates of much low adhesion strength induces the scattered growth of the oral squamous cell carcinoma cells through down-regulating the development of E-cadherin junctions despite the expression of functional E-cadherin, a hallmark of the epithelial phenotype (Figure 15).

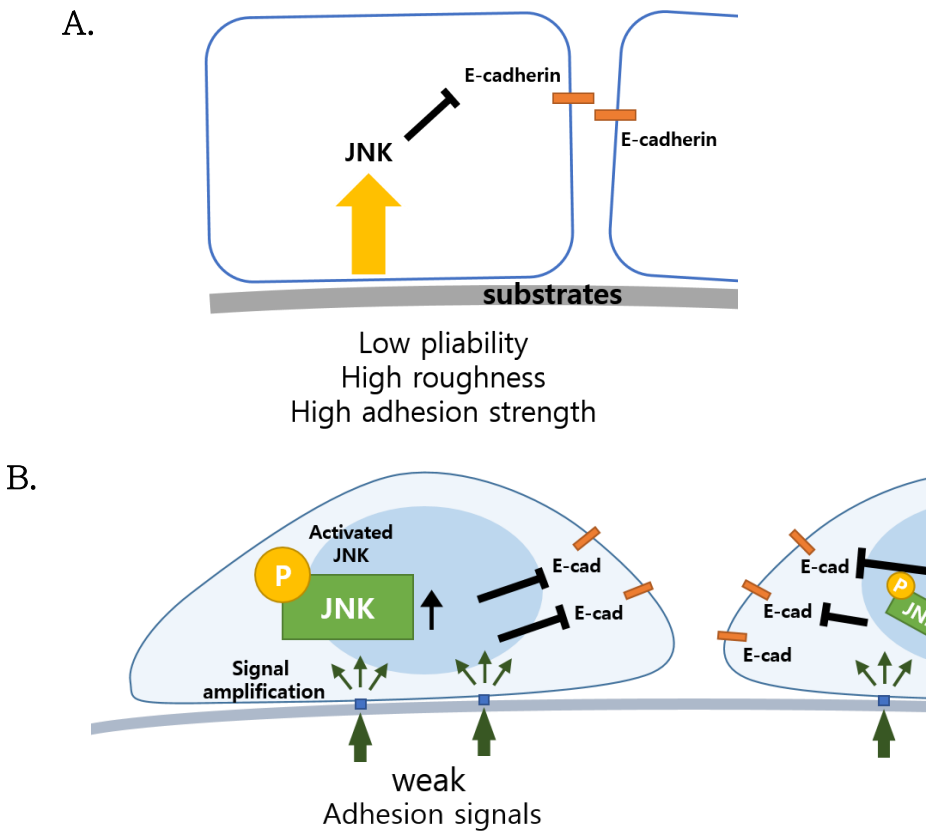

Figure 15. Summary of the findings. A) Substrate pliability, substrate roughness, and adhesion strength regulates the JNK activity which dissociates the E-cadherin junction of oral keratinocytes. B) Transformed cells characteristically over-stimulated JNK activity on the substrates of much low adhesion strength, which induces the scattered growth of the oral squamous cell carcinoma cells through down-regulating the development of E-cadherin junctions despite the expression of functional E-cadherin, a hallmark of the epithelial phenotype.

REFERENCES

1. Huntsman, D.G. and C. Caldas, *Assignment1 of the E-cadherin gene (CDH1) to chromosome 16q22.1 by radiation hybrid mapping.* Cytogenet Cell Genet, 1998. **83**(1-2): p. 82-3.
2. Semb, H. and G. Christofori, *The tumor-suppressor function of E-cadherin.* Am J Hum Genet, 1998. **63**(6): p. 1588-93.
3. Rushen, J., A.M. De Passille, and W. Schouten, *Stereotypic behavior, endogenous opioids, and postfeeding hypoalgesia in pigs.* Physiol Behav, 1990. **48**(1): p. 91-6.
4. Heymann, R., et al., *The characteristic cellular organization and CEACAM1 expression in the junctional epithelium of rats and mice are genetically programmed and not influenced by the bacterial microflora.* J Periodontol, 2001. **72**(4): p. 454-60.
5. Pizarro-Cerda, J. and P. Cossart, *Bacterial adhesion and entry into host cells.* Cell, 2006. **124**(4): p. 715-27.
6. Fleming, T.P., et al., *Assembly of tight junctions during early vertebrate development.* Semin Cell Dev Biol, 2000. **11**(4): p. 291-9.
7. Polyak, K. and R.A. Weinberg, *Transitions between epithelial and mesenchymal states: acquisition of malignant and stem cell traits.* Nat Rev Cancer, 2009. **9**(4): p. 265-73.
8. Berx, G., et al., *E-cadherin is a tumour/invasion suppressor gene*

mutated in human lobular breast cancers. EMBO J, 1995. **14**(24): p. 6107-15.

9. Berx, G., et al., *E-cadherin is inactivated in a majority of invasive human lobular breast cancers by truncation mutations throughout its extracellular domain.* Oncogene, 1996. **13**(9): p. 1919-25.

10. Becker, K.F., et al., *E-cadherin gene mutations provide clues to diffuse type gastric carcinomas.* Cancer Res, 1994. **54**(14): p. 3845-52.

11. De Leeuw, W.J., et al., *Simultaneous loss of E-cadherin and catenins in invasive lobular breast cancer and lobular carcinoma in situ.* J Pathol, 1997. **183**(4): p. 404-11.

12. Hibi, M., et al., *Identification of an oncoprotein- and UV-responsive protein kinase that binds and potentiates the c-Jun activation domain.* Genes Dev, 1993. **7**(11): p. 2135-48.

13. Baud, V., et al., *Signaling by proinflammatory cytokines: oligomerization of TRAF2 and TRAF6 is sufficient for JNK and IKK activation and target gene induction via an amino-terminal effector domain.* Genes & development, 1999. **13**(10): p. 1297-1308.

14. Rosette, C. and M. Karin, *Ultraviolet light and osmotic stress: activation of the JNK cascade through multiple growth factor and cytokine receptors.* Science, 1996. **274**(5290): p. 1194.

15. Kondoh, K. and E. Nishida, *Regulation of MAP kinases by MAP kinase phosphatases.* Biochim Biophys Acta, 2007. **1773**(8): p. 1227-37.

16. Byun, K., et al., *Heat shock instructs hESCs to exit from the self-renewal program through negative regulation of OCT4 by SAPK/JNK and HSF1 pathway.* Stem Cell Res, 2013. **11**(3): p. 1323-34.

17. Ip, Y.T. and R.J. Davis, *Signal transduction by the c-Jun N-terminal kinase (JNK)--from inflammation to development.* Curr Opin Cell Biol, 1998. **10**(2): p. 205-19.

18. Waetzig, V. and T. Herdegen, *Context-specific inhibition of JNKs: overcoming the dilemma of protection and damage.* Trends Pharmacol Sci, 2005. **26**(9): p. 455-61.

19. Bode, A.M. and Z. Dong, *The functional contrariety of JNK.* Mol Carcinog, 2007. **46**(8): p. 591-8.

20. Kiss, C., et al., *Assignment of the ARHA and GPX1 genes to human chromosome bands 3p21.3 by in situ hybridization and with somatic cell hybrids.* Cytogenet Cell Genet, 1997. **79**(3-4): p. 228-30.

21. Strutt, D.I., U. Weber, and M. Mlodzik, *The role of RhoA in tissue polarity and Frizzled signalling.* Nature, 1997. **387**(6630): p. 292-5.

22. Menke, A. and K. Giehl, *Regulation of adherens junctions by Rho GTPases and p120-catenin.* Arch Biochem Biophys, 2012. **524**(1): p. 48-55.

23. Ponik, S.M., et al., *RhoA is down-regulated at cell-cell contacts via p190RhoGAP-B in response to tensional homeostasis.* Mol Biol Cell, 2013. **24**(11): p. 1688-99, S1-3.

24. Schroeder, H.E. and M.A. Listgarten, *The junctional epithelium: from*

strength to defense. J Dent Res, 2003. **82**(3): p. 158-61.

25. Shimono, M., et al., *Biological characteristics of the junctional epithelium.* J Electron Microsc (Tokyo), 2003. **52**(6): p. 627-39.

26. Bosshardt, D.D. and N.P. Lang, *The junctional epithelium: from health to disease.* J Dent Res, 2005. **84**(1): p. 9-20.

27. Feghali-Assaly, M., et al., *Cytokeratin profile of the junctional epithelium in partially erupted teeth.* J Periodontal Res, 1994. **29**(3): p. 185-95.

28. Peters, B.H., et al., *Maintenance of cell-type-specific cytoskeletal character in epithelial cells out of epithelial context: cytokeratins and other cytoskeletal proteins in the rests of Malassez of the periodontal ligament.* Differentiation, 1995. **59**(2): p. 113-26.

29. Ye, P., et al., *Expression patterns of E-cadherin, involucrin, and connexin gap junction proteins in the lining epithelia of inflamed gingiva.* J Pathol, 2000. **192**(1): p. 58-66.

30. Wheelock, M.J. and P.J. Jensen, *Regulation of keratinocyte intercellular junction organization and epidermal morphogenesis by E-cadherin.* J Cell Biol, 1992. **117**(2): p. 415-25.

31. Lewis, J.E., P.J. Jensen, and M.J. Wheelock, *Cadherin function is required for human keratinocytes to assemble desmosomes and stratify in response to calcium.* J Invest Dermatol, 1994. **102**(6): p. 870-7.

32. Lewis, J.E., et al., *Cross-talk between adherens junctions and*

desmosomes depends on plakoglobin. J Cell Biol, 1997. **136**(4): p. 919-34.

33. Norvell, S.M. and K.J. Green, *Contributions of extracellular and intracellular domains of full length and chimeric cadherin molecules to junction assembly in epithelial cells.* J Cell Sci, 1998. **111 (Pt 9)**: p. 1305-18.

34. Presland, R.B. and B.A. Dale, *Epithelial structural proteins of the skin and oral cavity: function in health and disease.* Crit Rev Oral Biol Med, 2000. **11**(4): p. 383-408.

35. Lee, M.H., et al., *JNK phosphorylates beta-catenin and regulates adherens junctions.* FASEB J, 2009. **23**(11): p. 3874-83.

36. Lee, M.H., et al., *JNK regulates binding of alpha-catenin to adherens junctions and cell-cell adhesion.* FASEB J, 2011. **25**(2): p. 613-23.

37. Ridley, A.J. and A. Hall, *The small GTP-binding protein rho regulates the assembly of focal adhesions and actin stress fibers in response to growth factors.* Cell, 1992. **70**(3): p. 389-99.

38. Yang, S., et al., *Mechanisms by which the inhibition of specific intracellular signaling pathways increase osteoblast proliferation on apatite surfaces.* Biomaterials, 2011. **32**(11): p. 2851-61.

39. Yang, S. and H.M. Kim, *The RhoA-ROCK-PTEN pathway as a molecular switch for anchorage dependent cell behavior.* Biomaterials, 2012. **33**(10): p. 2902-15.

40. Essler, M., et al., *Pasteurella multocida toxin increases endothelial*

permeability via Rho kinase and myosin light chain phosphatase. J Immunol, 1998. **161**(10): p. 5640-6.

41. Wojciak-Stothard, B., et al., *Regulation of TNF-alpha-induced reorganization of the actin cytoskeleton and cell-cell junctions by Rho, Rac, and Cdc42 in human endothelial cells.* J Cell Physiol, 1998. **176**(1): p. 150-65.

42. Nishio, C., et al., *Expression pattern of odontogenic ameloblast-associated and amelotin during formation and regeneration of the junctional epithelium.* Eur Cell Mater, 2010. **20**: p. 393-402.

43. You, H., et al., *JNK regulates compliance-induced adherens junctions formation in epithelial cells and tissues.* J Cell Sci, 2013. **126**(Pt 12): p. 2718-29.

44. Rippere-Lampe, K.E., et al., *Mutation of the gene encoding cytotoxic necrotizing factor type 1 (cnf(1)) attenuates the virulence of uropathogenic Escherichia coli.* Infect Immun, 2001. **69**(6): p. 3954-64.

45. Orth, J.H., et al., *Substrate specificity of Pasteurella multocida toxin for alpha subunits of heterotrimeric G proteins.* FASEB J, 2013. **27**(2): p. 832-42.

46. Hauser, D., et al., *Comparative analysis of C3 and botulinal neurotoxin genes and their environment in Clostridium botulinum types C and D.* J Bacteriol, 1993. **175**(22): p. 7260-8.

47. Wagner, E.F. and A.R. Nebreda, *Signal integration by JNK and p38*

MAPK pathways in cancer development. Nat Rev Cancer, 2009. **9**(8): p. 537-49.

48. Bubici, C. and S. Papa, *JNK signalling in cancer: in need of new, smarter therapeutic targets.* Br J Pharmacol, 2014. **171**(1): p. 24-37.

49. Lee, G., H. Kim, and H.-M. Kim, *RhoA-JNK regulates the E-cadherin junctions of human gingival epithelial cells.* Journal of dental research, 2015: p. 0022034515619375.

50. Naydenov, N.G., A.M. Hopkins, and A.I. Ivanov, *c-Jun N-terminal kinase mediates disassembly of apical junctions in model intestinal epithelia.* Cell Cycle, 2009. **8**(13): p. 2110-21.

51. Shintani, Y., et al., *Collagen I promotes metastasis in pancreatic cancer by activating c-Jun NH(2)-terminal kinase 1 and up-regulating N-cadherin expression.* Cancer Res, 2006. **66**(24): p. 11745-53.

52. Lee, E.J., et al., *Characterization of newly established oral cancer cell lines derived from six squamous cell carcinoma and two mucoepidermoid carcinoma cells.* Exp Mol Med, 2005. **37**(5): p. 379-90.

53. Lei, K., et al., *The Bax subfamily of Bcl2-related proteins is essential for apoptotic signal transduction by c-Jun NH(2)-terminal kinase.* Mol Cell Biol, 2002. **22**(13): p. 4929-42.

54. Miyoshi, H., et al., *Development of a self-inactivating lentivirus vector.* J Virol, 1998. **72**(10): p. 8150-7.

55. Park, N.H., et al., *Immortalization of normal human oral keratinocytes with type 16 human papillomavirus.* Carcinogenesis, 1991. **12**(9): p. 1627-31.

56. Myong, N.H., *Loss of E-cadherin and Acquisition of Vimentin in Epithelial-Mesenchymal Transition are Noble Indicators of Uterine Cervix Cancer Progression.* Korean J Pathol, 2012. **46**(4): p. 341-8.

57. Zasadkevich, Y.M. and S.V. Sazonov, *[The role of E-cadherin cell adhesion molecule in human ontogenesis in norm and pathology].* Morfologiia, 2014. **146**(5): p. 78-82.

58. Zhang, X., et al., *N-cadherin expression is associated with acquisition of EMT phenotype and with enhanced invasion in erlotinib-resistant lung cancer cell lines.* PLoS One, 2013. **8**(3): p. e57692.

59. Hazan, R.B., et al., *Cadherin switch in tumor progression.* Ann N Y Acad Sci, 2004. **1014**: p. 155-63.

60. Derycke, L.D. and M.E. Bracke, *N-cadherin in the spotlight of cell-cell adhesion, differentiation, embryogenesis, invasion and signalling.* Int J Dev Biol, 2004. **48**(5-6): p. 463-76.

61. Sakurai, T., et al., *Loss of hepatic NF-kappa B activity enhances chemical hepatocarcinogenesis through sustained c-Jun N-terminal kinase 1 activation.* Proc Natl Acad Sci U S A, 2006. **103**(28): p. 10544-51.

62. Chang, Q., et al., *Sustained JNK1 activation is associated with altered histone H3 methylations in human liver cancer.* J Hepatol, 2009.

50(2): p. 323-33.

63. Hui, L., et al., *Proliferation of human HCC cells and chemically induced mouse liver cancers requires JNK1-dependent p21 downregulation.* J Clin Invest, 2008. **118**(12): p. 3943-53.

64. Vivanco, I., et al., *Identification of the JNK signaling pathway as a functional target of the tumor suppressor PTEN.* Cancer Cell, 2007. **11**(6): p. 555-69.

65. Ouyang, X., et al., *Activator protein-1 transcription factors are associated with progression and recurrence of prostate cancer.* Cancer Res, 2008. **68**(7): p. 2132-44.

ABSTRACT IN KOREAN

국문 초록

치은열구 상피를 포함하여 대부분의 구강상피는 상피의 대표적 특성인 E-cadherin 결합이 잘 발달된 반면에 치은염과 치주염과 밀접한 관계가 있는 치은접합상피(junctional epithelium)는 E-cadherin 결합의 발달이 미약하다. 따라서 구강상피의 E-cadherin 결합을 조절하는 기전을 이해하는 것은 병리생리학적으로 구강상피를 이해하는 데에 필수적이라 할 수 있다. 그러나 구강상피세포에서 E-cadherin 결합의 조절기전은 아직 잘 알려져 있지 않다. HOK-16B 치은각화상피세포주를 사용하여 구강각화상피 E-cadherin 결합 조절의 분자기전을 연구하였다. 구강상피세포의 E-cadherin 결합은 c-Jun N-말단 인산화효소(JNK)의 자극에 의해 발달이 억제되었으며 JNK 억제에 의해 발달이 촉진되었다. 이와 같이 구강각화상피의 E-cadherin 결합 발달을 억제하는 JNK는 small GTPase RhoA(RhoA)에 자극에 의해 p-JNK 발현이 증가하였고, RhoA 활성 억제에 의해 p-JNK 발현이 억제되었다. 이상의 결과는 구강각화상피세포의 E-cadherin 결합의 발달이 RhoA-JNK 신호전달에 의해 조절됨을 가리킨다. 한편, 접합상피는 다른 치은상피에 비해 미약한 E-cadherin 발현과 높은 p-JNK 발현을 보였는데, 이는 접합상피의 미약한 E-cadherin 결합의 발달이 p-JNK의 높은 발현과 연관되어 있을 가능성을 가리킨다. 상피성 종양세포가 세포간 결합을 상실하고 흩어지는 기전은 종양 발달의 초기 단계를 이해하는데 중요하다. 이에 E-cadherin을 발현하지만 일반 배양 조건에서 흩어져 증식하는 구강편평상피암세포주인 YD-10B 세포를 이용하여 구강편평세포암세포에서도 정상구강각화상피세포

와 마찬가지로 JNK에 의해 E-cadherin 결합의 발달이 조절되는지 연구하였다. YD-10B 세포는 정상세포인 HOK-16B 세포가 흩어지는 fibronectin 도포 기질 조건뿐만 아니라, 응집하여 세포결합을 형성하는 fibronectin 도포 조건 중 최대량의 fibronectin이 도포된 조건에서도 p-JNK가 강하게 발현하고 흩어져 증식하였다. 이와 같은 YD-10B 세포는 응집하는 극히 적은 양의 fibronectin 도포 기질 조건일지라도 JNK 활성을 자극하면 흩어졌고, 흩어지는 fibronectin 도포 기질 조건에서도 JNK 활성을 억제하면 응집하였다. 이상의 결과는 YD-10B 구강편평세포암세포가 기능적인 E-cadherin 발현의 상실의 결과가 아니라 JNK 활성에 의해 E-cadherin 결합의 발달이 억제됨을 가리킨다. 더불어서 이 결과는 YD-10B 암세포의 JNK 활성이 HOK-16B 정상 세포의 JNK 활성화 기질 부착 조건보다 약한 기질 부착 조건에서도 높게 활성화 되어 E-cadherin 결합 발달을 억제함으로써 YD-10B 세포가 정상세포와 달리 미약한 부착기질 조건에서도 흩어져 증식할 수 있음을 가리킨다. 이상의 결과로서 본 연구는 HOK-16B 정상구강각화상피세포와 YD-10B 구강편평세포암세포 모두 JNK 신호전달에 의해 E-cadherin 결합이 조절되어 세포간 결합이 저해될 수 있음을 보여 주었다.

주 요 어: E-cadherin, JNK, RhoA, 정상 구강잇몸세포, 구강편평상피암세포.

학 번: 2011-23828